TOTAL TEMPERATURE MEASUREMENT AT PULSE DETONATION ENGINE EXHAUST

by

NINAD RAMESH KAWLE

Presented to the Faculty of the Graduate School of

the University of Texas at Arlington in Partial

Fulfillment

of the Requirements

for the Degree of

MASTER OF SCIENCE IN MECHANICAL ENGINEERING

THE UNIVERSITY OF TEXAS AT ARLINGTON

MAY 2016

Acknowledgements

I take this opportunity to express my gratitude to all the people who have influenced and helped me, academically and personally. This thesis is the culmination of all those helping hands which made my efforts fruitful.

Dr. Frank K. Lu is a kind of mentor who guided me when it was most needed and gave me enough liberty to pursue my research without any hindrances. I can never forget all the discussions we had, academic or otherwise, which helped me grow as an independent researcher and as a human being. I consider myself very fortunate that I got a chance to work under such a mentor whose high work expectations helped me hone my skills and elevate my work ethics.

I feel obliged towards my thesis committee members, Dr. Donald Wilson and Dr. Ankur Jain, for agreeing to be part of my committee and for the insightful feedback of my work. I would like to thank Dr. Dibesh Joshi and Dr. Raheem Bello for the guidance and all the thoughtful advices which helped ease my foray into experimental world. I would also like to thank Mr. David Carter for all the support in setting up my experimental as well as in conducting experiments while making sure I abide by the safety norms.

I dedicate this thesis to my parents Seema and Ramesh Kawle for wholeheartedly supporting my ambitions while keeping my feet grounded. I would like to thank my friends back in India for their sense of support. The thesis would have never been possible without all the encouragement and help provided by my friends Sudheer, Umang, Saif, Adeetya, Atul and Sushma throughout my stay here at UTA.

May 4, 2016

Table of Contents

Abstract

TOTAL TEMPERATURE MEASUREMENT AT PULSE DETONATION ENGINE EXHAUST

by

NINAD RAMESH KAWLE, M.S.

The University of Texas at Arlington, 2015

Supervising Professor: Frank K. Lu

Pulse detonation engines (PDEs) are being studied in recent years as a potential means of power production. In PDEs, a supersonically travelling detonation wave traverses through the detonation tube. One of the parameters that has not been properly measured to date is the total temperature of the exhaust of the PDE. The objective of the research was to calibrate and employ miniature type E thermocouples for exhaust temperature measurement of the PDE. The probe making process along with the dynamic calibration techniques for the bead thermocouples are discussed. The time constants for thermocouples were determined. Reactive mixture containing hydrogen and oxygen was used in the pulse detonation engine. The exhaust pressure was also measured. The exhaust temperature recorded was vastly different from theoretical predictions. It is hypothesized that radiation losses are the major reason for cooling of jet plume causing the drop in temperature. A shielded enclosure to mitigate radiation losses is recommended.

List of Illustrations

List of Tables

Chapter 1

Introduction

Pulse detonation engines (PDEs) are being studied in recent years as a potential means of power production and as a replacement for jet propulsion devices. [1][2] The main difference between a traditional internal combustion engine and a PDE is that the fuel in the IC engine undergoes deflagration whereas detonations take place in the PDE. The PDE is advantageous over IC engines for reasons such as higher thermodynamic efficiency, high power-to-weight ratio and reduced number of moving parts as well as ease of manufacturing and compactness. [3] The basic methodology of a PDE follows ignition of a detonable mixture either by an external device such as a spark plug or by inducing a weak shock wave from another source.

1.1 Pulse Detonation Engine [4]

Combustion is a chemical reaction between a fuel and an oxidizer. Commonly, combustion arises with hydrocarbons as the fuel and air as the oxidizer. There are two classes of combustion: the commonly encountered deflagration and detonation. A deflagration wave travels subsonically through the reactants. On the other hand, the supersonically traveling detonation wave is actually a shock wave which perpetuates because of the energy released from chemical reactions. These reactions occur from the increase in enthalpy from shock compression of the reactants. The detonation mode of the traversing flame has a minimum entropy increase. [3]

The pulse detonation engine operates as per the cycle shown in Figure 1.1, wherein the major processes are purging, fuel injection and ignition followed by detonation wave propagation. Before the start of the fuel injection process, the detonation tube is at ambient conditions. During fuel injection, the detonation tube is filled with fuel and oxidizer through valves. The duty cycle, which can be defined as the amount of time the valves are kept open, is decided based upon the operating frequency of the engine as well as the filling fraction. The operating frequency of the PDE can be defined as, the number of times the PDE cycle is repeated in a second. The filling fraction is defined as the ratio of the volume of the detonation tube which is filled with the oxidizer and fuel mixture over the total available volume.

Once the fuel and oxidizer are injected in the detonation tube, the mixture is ignited typically with the help of spark plugs. The ignition initiates deflagration which turns into a propagating detonation wave over the deflagration-to-detonation (DDT) length. When the detonation wave exits the detonation tube, it induces an expansion wave towards the closed end of the tube. The exhaust is followed by the purge air process which scavenges the residual fuel out of the tube and the cycle repeats.

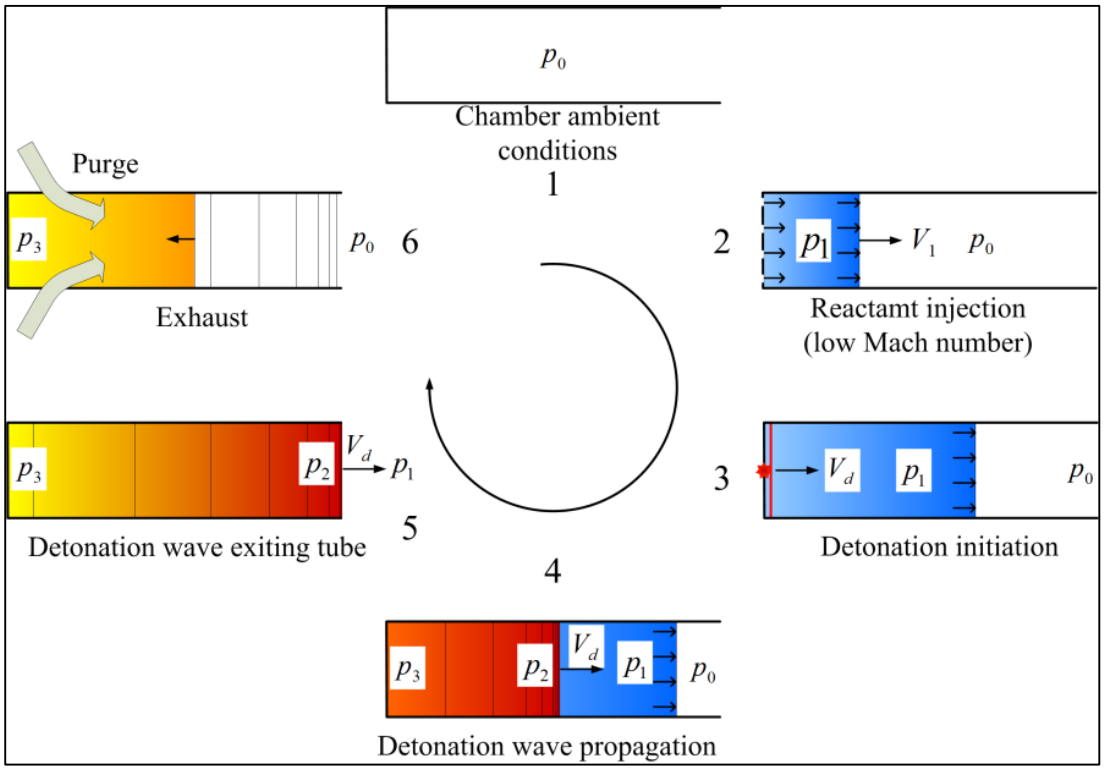

Figure 1.1: Stages of PDE cycle [4]

1.2 Total Temperature [5]

The total temperature, also known as the stagnation temperature, at the exhaust of the PDE is not well-known. Figure 1.2 depicts the one-dimensional combustion wave in a wave-fixed reference frame.

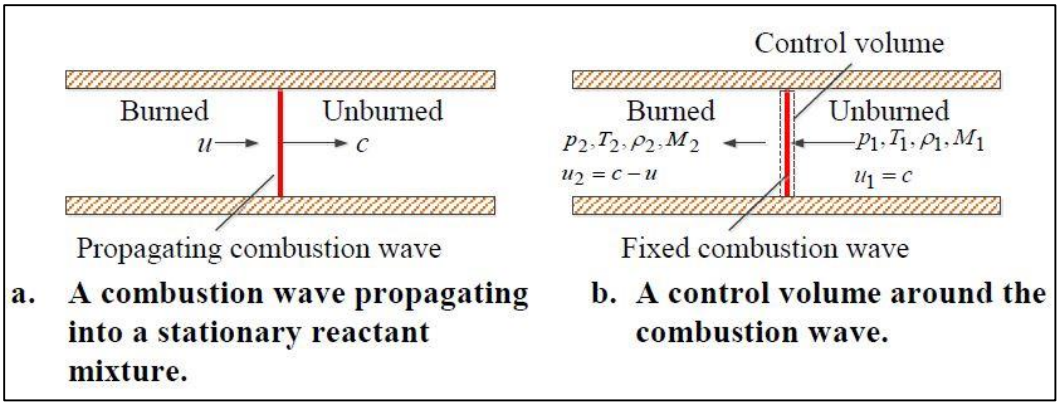

Figure 1.2: One-dimensional combustion wave in a wave-fixed reference frame [1]

Consider Figure 1.2.b; let the sections of unburned gases and burned gases in the wave-fixed reference frame be denoted by 1 and 2 respectively. The total temperature can be derived from the simplified form of the energy equation with adiabatic condition which can be given as,

$$h_1 + \frac{u_1^2}{2} + q = h_2 + \frac{u_2^2}{2} \tag{1.1}$$

where h is enthalpy, q is heat release per unit mass from the combustion process and u is velocity. For a calorifically perfect gas, the relation between enthalpy and static temperature can be given by, $h = c_p T$, where c_p is the specific heat at constant pressure and T is the temperature. For a calorically perfect gas, equation (1.2) then becomes

$$c_p T_1 + \frac{u_1^2}{2} + q = c_p T_2 + \frac{u_2^2}{2} \tag{1.2}$$

When the fluid is slowed down to the stagnation condition, equation (1.2) further reduces to

$$c_p T + \frac{u^2}{2} = c_p T_0 \tag{1.3}$$

where T_0 is known as the stagnation temperature. Equation (1.3) can be further simplified by substituting the relations for the specific heat at constant pressure in terms of γ ratio of specific heats and the Mach number

$$M = \frac{u}{a} \tag{1.4}$$

and

$$c_p = \frac{\gamma R}{\gamma - 1} \tag{1.5}$$

where the speed of sound is given by

$$a = \sqrt{\gamma R T} \tag{1.6}$$

with R the gas constant. The reconstitution of equations (1.4), (1.5) and (1.6) leads to the final equation for the total temperature of a calorically perfect gas

$$\frac{T_0}{T} = 1 + \frac{\gamma - 1}{2} M^2 \tag{1.7}$$

1.3 Methodology

The methodology section describes the approach taken for conducting calibration experiments and measurement experiments. It also discusses the error fraction approach, which is the solution of a homogeneous first-order differential equation and which was used to find out the response time of the thermocouple.

1.3.1 - Thermocouple Calibration Experiment

The thermocouple calibration experiment consisted of applying a step temperature change to the thermocouple to evoke a step response from the thermocouple. The recorded data was then used to obtain the response time of the thermocouple. The time constants of type E thermocouples were calibrated before they were used for the total temperature measurement. Three gauges of thermocouples were used, namely, AWG 20, 24 and 50 corresponding to wire diameters of 0.032, 0.0201 and 0.001 in.[1]

[1] AWG = American wire gauge.

Two methods were used to apply a step temperature change. The first method used hot water as a heat source. Water was heated with the help of a hot plate till it reached the boiling point. In order to capture the temperature change observed by the thermocouple, an NI PXI-1042Q data acquisition system was used. A LabVIEW program was created which accepts the output from the thermocouple as a voltage and writes the data file. The LabVIEW interface converts the output in voltage into the temperature depending upon the type of thermocouple. After selecting the type E thermocouple and defining the path where the data file was to be saved, the room temperature was manually entered as the cold junction temperature.

The room temperature was measured with the help of a non-contact infrared thermometer (Omega). The values for number of samples per second and the total number of sample points were entered before the start of the experiment. Acetone, which works as a cleaning agent, was dropped on the tip of the thermocouple to remove any impurities. The recording of the data was then started. The temperature change was applied by dropping hot water on the tip of the thermocouple with the help of a pipette. The data file was then copied into Microsoft Excel for further use.

The second method for the temperature change used cold water. Ice cubes were kept in an insulated container on which salt was sprinkled to bring the temperature down. Cold water was then poured on top of the ice- salt mixture which cooled the water down to a subzero temperature. The cold water was then used to apply a step temperature change. There was no change in data acquisition procedure.

1.3.2 – Error fraction approach

The curve fitting approach involves finding the starting point at which the curve starts rising or falling, depending on the type of input. But, this approach is not always feasible for cases in which the data fluctuates excessively in a range. The nature of the thermocouple output depends on its sensitivity. The sensitivity as well as the response time of the thermocouple are based upon different parameters such as type of thermocouple and thickness of thermocouple wires. Finding the point at which the step change input was applied to the thermocouple is important as the nature of the equation given below depends on the starting point.

The error fraction approach is derived from the first-order nature of the thermocouple which is represented by the equation which can be given as follows:

$$e^{-\frac{t}{T}} = \frac{y_t - y_{\infty}}{y_0 - y_{\infty}} = \Gamma(t) \tag{1.8}$$

where $\Gamma(t)$ is error fraction of the output, y_t is value of the function at that time instance, y_0 is the initial value of the function and y_{∞} is the steady state value.

The time constant of a first-order system is the time required for the function to reach 63.2% of the steady-state value. The time constant can be found by applying an exponential fit to the output curve for the step input. In case of error fraction approach, as shown in Figure 1.2, the curve starts from 1 and decreases linearly till the steady state value of the function is reached. Hence, an exponential fit can be applied to the curve with the help MATLAB or Microsoft Excel to find the time constant.

1.3.3 Pressure and stagnation temperature measurement:

The pressure data is one of the means of confirming whether the detonation occurred inside the PDE tube or not. A series of pressure transducers were installed along the length of the PDE tube with the first one being 20 cm away from the closed end of the PDE tube. Four more pressure transducers were installed 10 cm apart from each other. These equidistant pressure transducers (PCB: 111A24) were numbered from 1 to 5 starting from the closed end of the detonation tube. The data only from transducers 4 and 5, which measures pressure just before the detonation wave exits from detonation tube, was recorded. This was done as the data file size had be constrained because of the high sampling rate. The wedge attached to the arm, as shown in Figure 1.3, had one pressure transducer located recessed within a stagnation tube at the center of the flow.

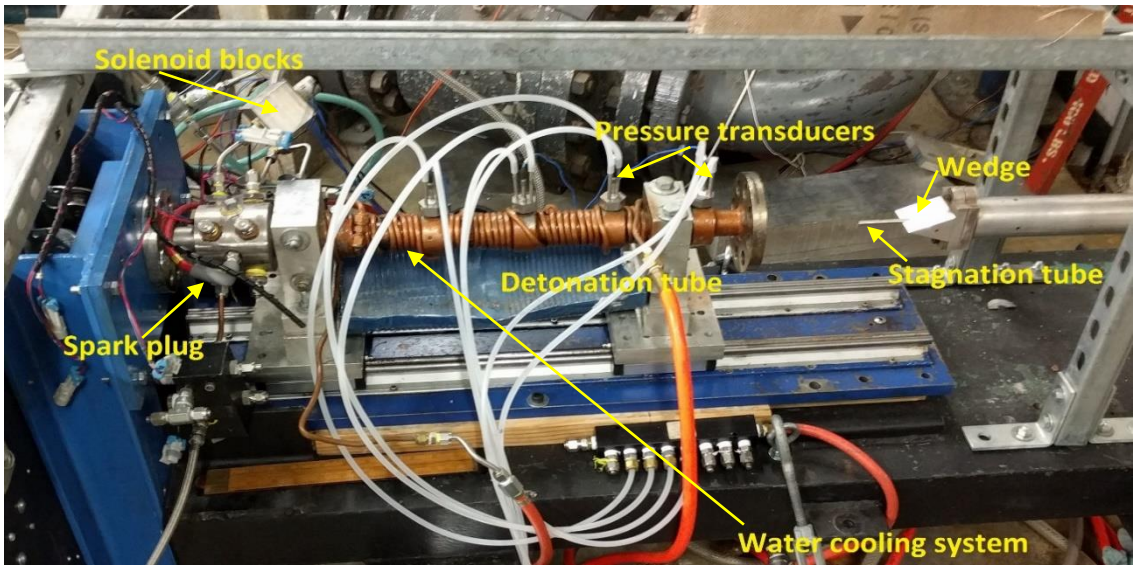

Figure 1.3: Pulse detonation engine setup. The total temperature probe mounted inside stagnation tube is seen on the right

This was done because of the small diameter of the tube. The sampling rate depends on the capacity of the data acquisition system as well as the maximum number of sample points that can be amassed. It was done to ensure that the data acquisition lasts for the predefined time during the detonation engine run enabling us to capture the detonation wave characteristics. The data from this pressure transducer was collected with the help of LabVIEW program. The sampling rate was usually varied between 400K samples per second to 880K samples per second.

The stagnation temperature measurement was done by modifying the setup of exhaust stagnation pressure measurement. The wedge that houses the pitot tubes was replaced by a new a wedge which replicated the same design as shown in Figure 1.3. The new stagnation tube designed to house the thermocouple probe was then fitted inside the new wedge. The LabVIEW program was altered to acquire data from thermocouple.

Chapter 2

Design and Setup

The total temperature measurement involved modifying the existing pulse detonation engine setup and the use of devices such as data acquisition system for the thermocouple calibration experiment as well as the exhaust temperature measurement experiment. The existing setup only had an arrangement for pressure measurement and hence a stagnation tube that houses the thermocouple probe was designed. Also, the wedge to accommodate the stagnation tube was manufactured. This wedge replicates the design of wedge for pressure transducers. The thermocouple, being very delicate, was handled with care. Before making the actual probe, various dry runs were done and guidelines were created to facilitate the easy handling of the thermocouple. Hence, the procedure for the thermocouple probe creation has been discussed at length along with the setup description for the thermocouple calibration as well as the exhaust pressure and temperature measurement experiments.

2.1 Total Temperature Probe

Total temperature measurements were done by attaching the thermocouple probe at the exhaust of an existing pulse detonation engine setup. Pressure measurements at the engine exhaust were done by pressure transducers. The arrangement for it included recessed mounted pressure transducers installed at the end of pitot tubes which in turn were incorporated inside a sharp wedge. The same wedge design was replicated for the thermocouple probe with modification for housing the thermocouple probe along with the stagnation tube in the same setup. Figure 2.1 depicts the CAD drawing of the wedge which was fabricated in-house at the UTA machine shop. The center orifice was big enough to press fit the stagnation tube and hence no other provision was required to hold the tube in place. The wedge was machined from an aluminum (Type 6061) block.

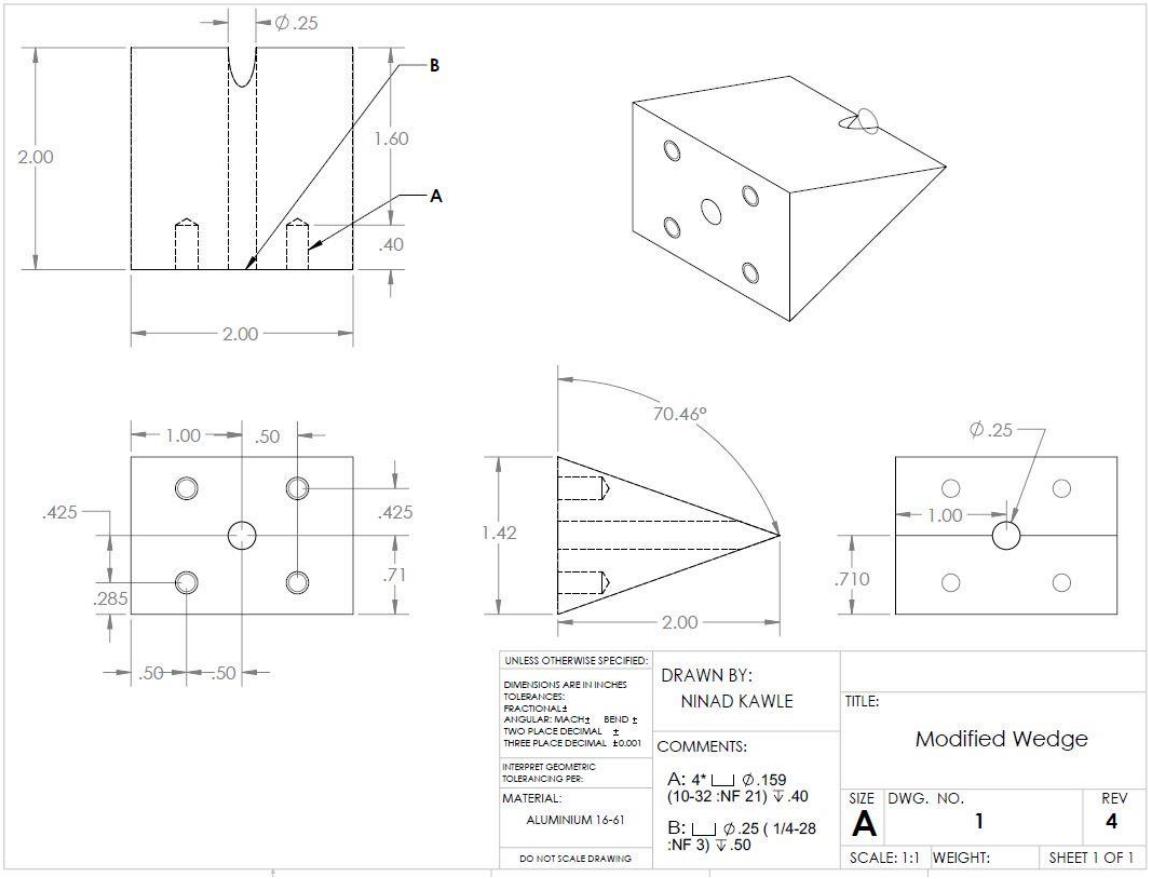

Figure 2.1: CAD drawing of the wedge which houses the stagnation tube

2.2 Stagnation Tube Design

Two salient factors of the stagnation temperature tube design were the ratio of the exit vent to the entrance area and the distance between the tip of the thermocouple and the stagnation tube entrance. In order to determine what would be the best design, different geometries of the stagnation tube were created for different area ratios. Bontragger [6] advised the vent to entrance area ratio to be 20%. The geometries were modified by altering the distance between the tip of the thermocouple from the entrance of the tube, keeping Bontragger's recommendations in mind. Hence, different geometries with the distance of the thermocouple tip from the inlet, starting from 0.04 in. to 0.09 in. and increasing in steps of 0.01 in. were made for the area ratio of 20%. The geometries were further modified by increasing the distance of the tip of the thermocouple from entrance by steps of 0.1 in. till the 1 in. mark and then at 1.5 in. and 2 in. from the stagnation tube

entrance. In order to verify what area ratio is better, geometries with area ratios of 30, 40 and 50% were also created. These geometries had the tip of the thermocouple 0.1 in. away from the stagnation tube entrance. Like the geometries with exit vent area to entrance area ratio of 20%, the geometries created with area ratios of 30, 40 and 50% were further modified with tip of the thermocouple being at 0.3, 0.5 and 1 in. away from the stagnation tube entrance.

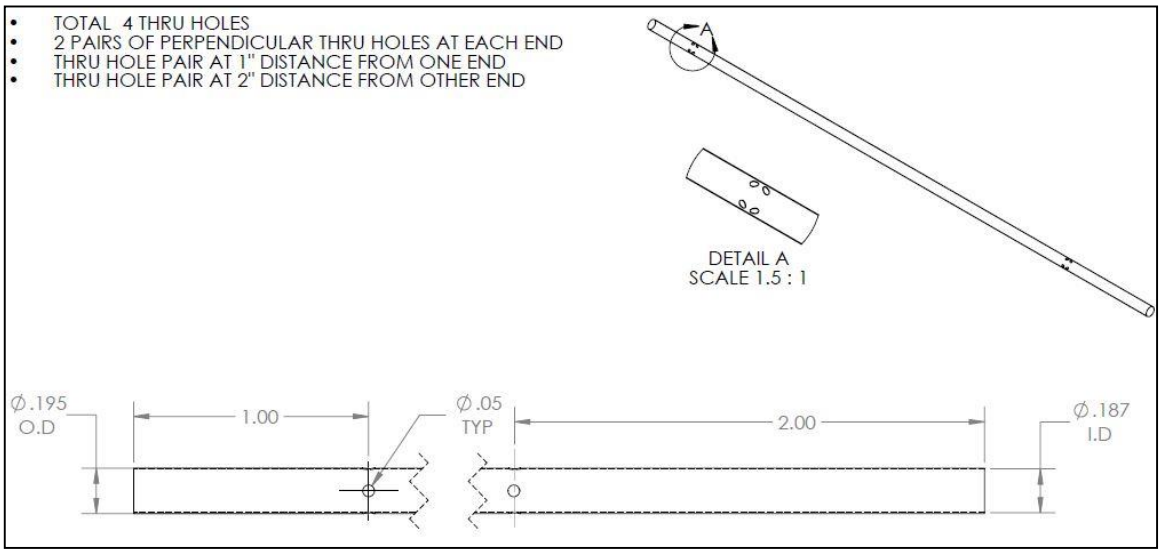

Figure 2.2: CAD drawing of stagnation tube which houses the thermocouple probe

The design depicted in Figure 2.2 was selected after running the simulations. The stagnation tube was 5 in. long with the exit-to-entrance area ratio of 30%. The exit holes were drilled at 1 in. as well as 2 in. from both the stagnation tube ends. This provision ensured flexibility for recessing the thermocouple in the stagnation tube at various distances from the stagnation tube entrance.

2.3 Setup–Thermocouple Probe Preparation

The type E thermocouple was used in the experiment. It has an operating temperature range of −270 °C to 1000 °C. The diameter of the thermocouple wires was chosen to be 0.001

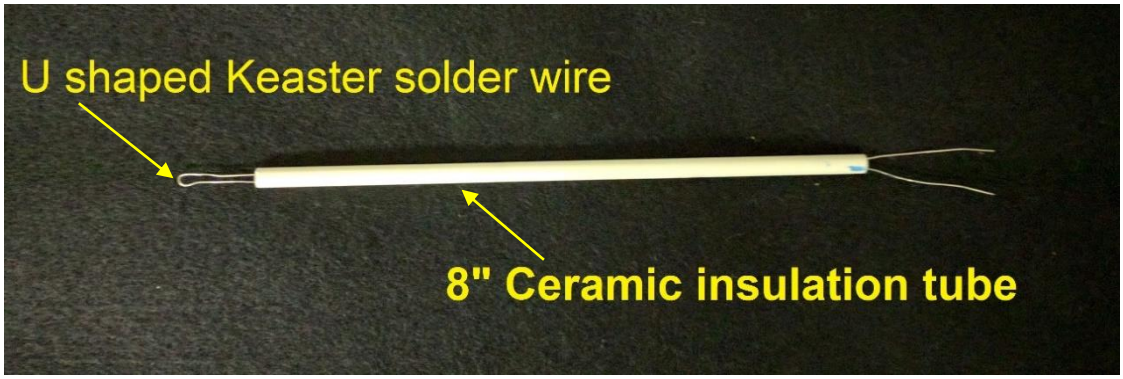

Figure 2.3: U-shaped holder made from solder wire to get the thermocouple through the shown Ceramic insulation tube

in. to achieve a faster response. [7] Latex gloves were worn at all times while handling the thermocouple to avoid any contamination. A four-hole ceramic insulation tubing (Omega FRM-364316) was used to house the bare thermocouple wires. The tubing has a 3/16 in. outer diameter and has four inner tubes with 3/64" in. diameter. Solder wire molded into a 'U' shape, as shown in Figure 2.3, was then passed into two of the ceramic tube orifices. Solder wire was used as a means to get tiny thermocouple wires through the ceramic insulation tubing. Keaster 60/40 Rosin core wire was selected after several dry runs of the procedure as it is malleable as well as strong enough to carry the thermocouple wire through the holes. The ceramic tubing as well as solder wire were first dipped in acetone to clean them.

The bare thermocouple was taken under the magnifying glass for better viewing and inserted into the ceramic tube without taking the thermocouple off of the supporting cardboard package. Gently one of the stickers at the end of thermocouple was pulled off with the help of tweezers. The end was then put on the solder wire and some cyanoacrylate (superglue) was put on the connection to fix it. The same action was repeated to the other thermocouple wire. After the glue dried, the other ends of solder wires at the loop were gently pulled so that both connections moved at once. The connections were cut once both the thermocouple wires were out of the other end of ceramic tubing. Silicone gel was applied at the entrance of the holes through which thermocouple wires were passed ensuring that the thermocouple bead was at the

required distance. A copper rod with sharp end was used to evenly spread the silicone gel on the ceramic tube holes to hermetically seal them. The silicone gel was left untouched overnight to get cured completely. The open ends of the thermocouple were connected to the chromel (90% nickel + 10% chromium) and constantan (55% copper + 45% nickel) extension wires (Omega PR-E-24-25) which are of the same material as that of the type E thermocouple wires. The thermocouple wire and extension wire were first connected together with the help of cyanoacrylate. In order to ensure the proper connection established, the thermocouple wire was then wound over the extension wires and then the connection was soldered. The same procedure was repeated with the other thermocouple wire. The connections were enclosed inside heat shrink tubing in order to avoid any kind of exposure and contamination. The whole assembly was then placed onto a V-block.

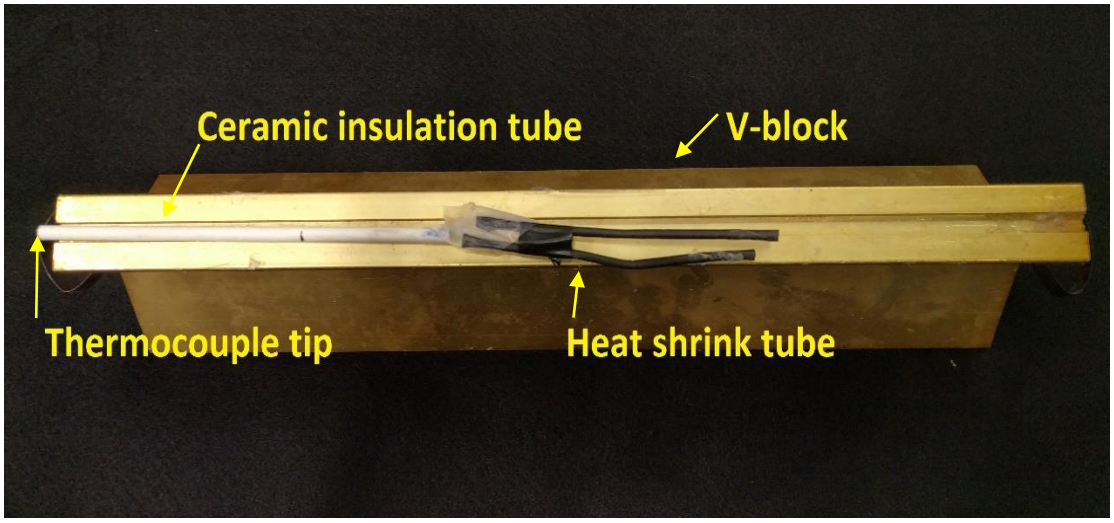

Figure 2.4: Thermocouple probe kept on the V-block with heat shrink tube over the bare Type E (0.001-inch diameter) thermocouple wires

2.4 Thermocouple Calibration Experiment

Calibrations were performed to determine the time constant of the thermocouples. Two different setups were used for the calibration experiments which included using two different data

acquisition systems, NI PXI-1042Q and NI PXI-1065Q. The NI-PXI 1042Q could amass data at the maximum sampling rate of 1.25 million samples per second per channel simultaneously maximum for 8 channels while the NI PXI-1065Q offers a higher sampling rate of 2.5 million samples per second per channel simultaneously maximum for 8 channels. The NI PXI-1042Q system, as explained in the methodology section of chapter 1, was used to record data from type E thermocouples whereby the thermocouples AWG 20 and AWG 24 were connected to the breadboard NI SCB-68. The breadboard was then connected to the data acquisition system. The non-contact thermometer (Omega), as shown in Figure 2.5, is an infrared thermometer which was used to measure the room temperature. The thermometer gauges the temperature by infrared rays and displays the temperature in Celsius or Fahrenheit as per the user's choice. The recorded temperature was then input as the cold junction temperature for the thermocouple.

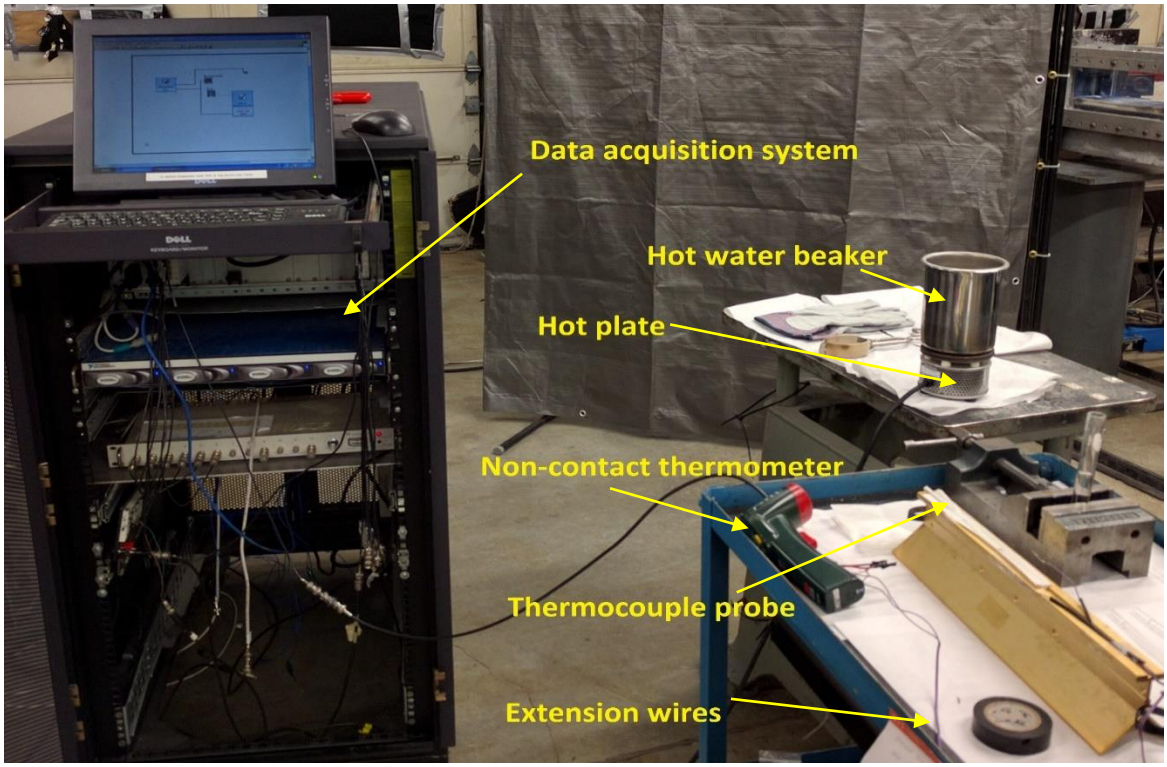

Figure 2.5: Calibration experiment setup with hot water as a heat source

The beaker on the hot plate, as shown in Figure 2.5, contained hot water which was being used as a means of producing the step response from the thermocouple with the step temperature change being applied by dropping the hot water on the tip of the thermocouple. The same experiment was again repeated with the 0.001 in. diameter type E thermocouple with the NI-PXI 1065Q data acquisition system. The extension wires were connected to the NI-PXI 1065Q with the help of a wire-to-BNC connector. The connection between extension wires and the wire-to-BNC connector serves as the cold junction.

2.5 Total Temperature Measurement

The pulse detonation engine is a perfect example of controlled detonations in a restricted environment. The pulse detonation tube that was used is 26 in. (660 mm) long with an inner diameter of 1 in. (25.4 mm). The outer diameter of the PDE tube is 1.5 in. (38.1 mm).

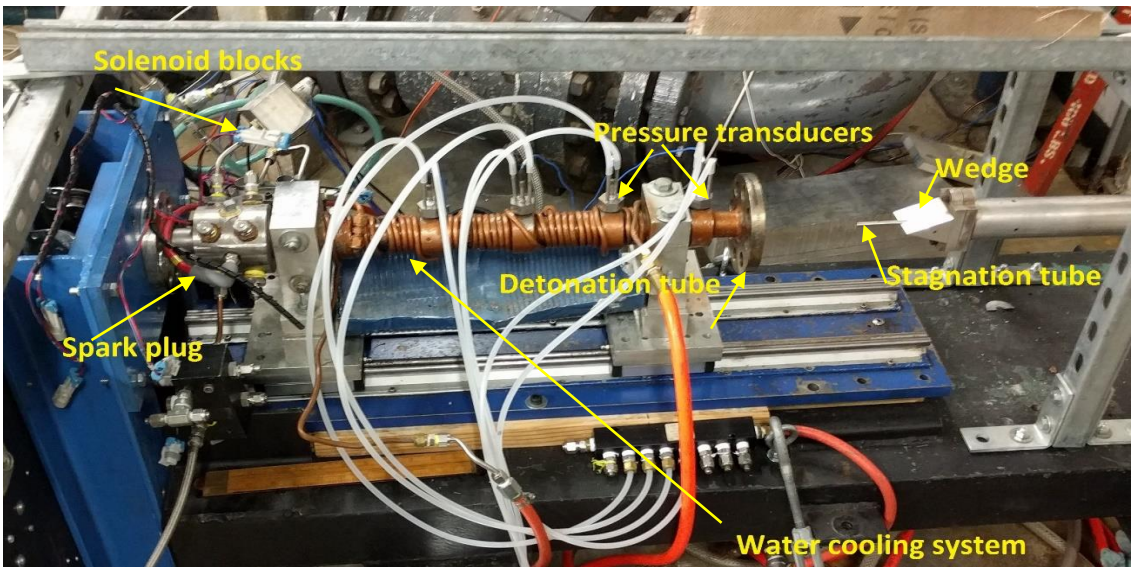

Figure 2.6: Pulse detonation engine setup. The total temperature probe mounted inside stagnation tube is seen on the right

The fuel and oxidizer were injected into the combustion chamber with the help of solenoid valves. An automotive spark plug was used as an igniter after the purge air and fuel injection

phases were completed. The solenoid valves were controlled through the LabVIEW program which controlled the duty cycle of the solenoid valves. The duty cycle is the amount of time for which the solenoid valve is kept open so that the stipulated amount of fuel or oxidizer will be injected inside the detonation tube. The duty cycle is calculated based upon the maximum mass flow rate available for the solenoid valve and the frequency at which the pulse detonation engine is run. [8] A DC power supply and buffer amplifier were used to power and trigger the solenoids respectively. The fuel lines were connected to the gas cart which comprises of pneumatic check valves and flash arrestors through which fuel and oxidizer were fed to the solenoid valves. BNC cables from pressure transducers (Model: PCB 111A24) were connected to the DAQ NI PXI-1042Q. The copper tubes, as shown in Figure 2.6, were part of water cooling system which helped keep the detonation tube cool.

The second leg of the experiment consisted of measurement of the total temperature with the use of Type E thermocouple probe. The thermocouple assembly, shown in Figure 2.4, was inserted inside the stagnation tube. The stagnation tube was then press fitted inside the new wedge which replaced the existing wedge which housed pressure transducers. The extension wires coming from the thermocouple were connected to the NI-PXI 1065Q data acquisition system with the help of a wire-to-BNC connector. The connection between the extension wires and the wire-to-BNC connector was wrapped with an aluminum foil that acted as a shield to mitigate any electromagnetic interference.

Chapter 3

Numerical Analysis

The stagnation temperature tube (more briefly called the stagnation tube) was one aspect of making the thermocouple probe. The stagnation tube housed the thermocouple probe. Two salient features of the stagnation tube design were the location of the thermocouple tip from the stagnation tube entrance and exhaust area to entrance area ratio. ANSYS Fluent was used to aid in selection of the stagnation tube design. The NASA CEA applet [11] and 'Compressible Aerodynamics Calculator' from Virginia Tech [12] were used to find normal shock relations.

3.1 – Shock Tube Relations

A detonation wave is a shock wave which traverses through the mixture of reactants because of the chemical energy which is released when the reactive mixture undergoes chemical reactions. [4]

The pulse detonation engine tube was treated as a shock tube which was filled with reactive mixture. Hydrogen as a fuel and oxygen as an oxidizer were assumed. The normal shock tube relations were then found out by using NASA CEA. The website hosts an online chemical equilibrium applet which can calculate shock tube relations, CJ detonation parameters and combustion properties.

At ambient pressure and 300 K temperature, the stoichiometric oxyhydrogen detonation velocity was 2835.4 m/s. The detonation wave exits the tube as a shock wave (more strictly called a blast wave). An expansion wave propagates towards the closed end of the tube.

For simplicity, ignoring the expansion wave, the relative Mach number with which the wave travels through the ambient air, is given as

$$M_1 = \frac{V_1}{a_1} = \frac{V_1}{\sqrt{\gamma R T_1}} \tag{3.1}$$

$$M_1 = \frac{2850}{\sqrt{1.4 \times 286 \times 300}} = 8.196 \tag{3.2}$$

The Virginia Tech applet was used for the calculation of normal shock relations. At the detonation tube exit interface, the shock wave temperature T_2 was calculated as 3330.5 K. Wave velocity V_2' and pressure P_2 turned out to be 386.86 m/s and 83.4 bar respectively. The velocity of air and the corresponding Mach number were computed as follows.

$$V_2' = \mathrm{c} - V_2 = 2448\ m/s \tag{3.3}$$

$$M_2 = \frac{V_2'}{a_2} = \frac{V_2'}{\sqrt{\gamma R T_2}} \tag{3.4}$$

$$M_2 = \frac{2448}{\sqrt{1.4 \times 286 \times 3330}} = 2.12 \tag{3.5}$$

One more steady shock was assumed before the wave enters into the stagnation tube. NASA CEA applet was used to compute the required values for which temperature T_3 turned out to be 4678.88 K. Wave velocity V_3 and pressure P_3 were 629.48 m/s and 478.3 bar respectively.

Along with these calculated values, values obtained from exhaust pressure measurement experiments done at PDE exhaust were used as reference. But, the reference values were found to be too high for the stagnation tube geometry and hence another approach had to be adopted for the selection of stagnation tube geometry.

3.2 – Geometry Creation and Mesh Generation

As outlined in chapter 1, two-dimensional geometries of the stagnation tube were created using Pointwise™. The channel representing the stagnation tube width was 0.195 in. The thermocouple was created inside the tube with the help of 'connectors'. The pressure far-field was created outside the tube.

The exhaust vent diameter was decided by considering the different area ratios between vent area and inlet area. This area ratio was varied between 1:5 to 1:2. Accordingly, different geometries were created for different area ratios The geometries were modified by altering the distance between the tip of the thermocouple from the entrance of the tube, keeping Bontragger's recommendations in mind [6]. Hence, different geometries with the distance of the thermocouple tip from the inlet, starting from 0.04 in. to 0.09 in. and increasing in steps of 0.01 in. were made for the area ratio of 20%. The geometries were further modified by increasing the distance of the tip of the thermocouple from entrance by steps of 0.1 in. till the 1 in. mark and then at 1.5 in. and 2 in. from the stagnation tube entrance. In order to verify which area ratio is better, geometries with area ratios of 30%, 40% and 50% were also created. These geometries had the tip of the thermocouple 0.1 in. away from the stagnation tube entrance. Like the geometries with exit vent area to entrance area ratio of 20%, the geometries created with area ratios of 30%, 40% and 50% were further modified. The tip of the thermocouple for these area ratios was at 0.3, 0.5 and 1 in. away from the stagnation tube entrance.

3.3 – Solver Settings

3.3.1 Assumptions for modelling

The flow was assumed to be an unsteady turbulent flow and solved using pressure solver.

3.3.2 Simulation setup

The simulation was done by first creating the stagnation tube geometry in the Pointwise™ software. The geometry was then imported to the ANSYS Fluent by exporting it to CAE. Table 3.1

illustrates the basic simulation setup settings and Table 3.2 depicts the solution methods which were adopted for the simulation.

Table 3.1: Basic settings of CFD simulation

Parameters/Models	Settings
Spatial and Time settings	2-D Simulation Gravity disabled
Solver	Pressure based solver Absolute velocity formulation Steady state analysis
Turbulence model	Standard k–ε

Table 3.2: Solution Methods

Setting Solution Methods	Settings
Pressure-Velocity coupling	Simple
Gradient	Least squares cell based
Pressure	Standard
Momentum	First order upwind
Volume Fraction	First order upwind
Turbulent kinetic energy	First order upwind
Transient Formulation	First order implicit

3.3.3 Boundary conditions

The inlet was chosen as ‘velocity inlet’ for which velocity, pressure as well as the temperature were given as input. The pressure far field boundaries were considered the ‘pressure outlet’ to avoid predicting the exhaust pressure at the exit area. The area other than the exhaust vents was assigned ''wall’ boundary conditions. The thermocouple was modeled and attributed ‘wall’ boundary condition. The exhaust vents modeled were made as ‘connections’ boundary condition. Table 3.3 portrays the basic boundary conditions which were attributed to the geometry. To save computational time, geometries made for exhaust to inlet ratio of 30%, 40% and 50%, were not made completely. Only the upper portion of these geometries was created and ‘symmetry’ condition was implemented.

Table 3.3: Boundary conditions

Boundary Conditions	Settings
Inlet	Mixture: Uniform inlet velocity of 10–280 m/s in increments of 20 m/s
Symmetry	For geometries with only the upper domain
Stagnation tube wall	Wall
Thermocouple tip	Wall
Ends of outside domain	Pressure Outlet
Exhaust vents	Left as Connections

3.4 Convergence Criteria and Computational Results

The residuals are imbalance between linearly discretized equations. The residual monitors were lowered by the factor of 10^{-6} to check whether the residual plot follows a linear path. The initial guess for the velocity and temperature were 10 m/s and 300 K respectively. The initial pressure was 1.012 bar. The velocity was increased in the increment of 20 m/s till divergence by temperature was detected. Different geometries with varying area ratios and different thermocouple locations were tested.

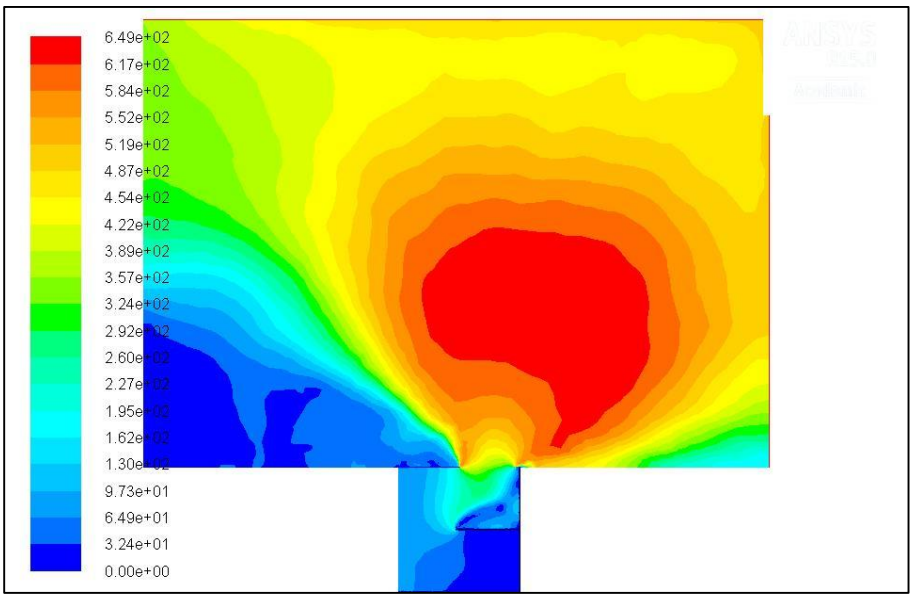

Figure 3.1: Velocity contour for the stagnation tube geometry with 1 exhaust vent

Figure 3.1 depicts the velocity contour for the two-dimensional stagnation tube geometry. The Figure represents the divergence condition for the inlet velocity of 120 m/s. Figure 3.2 illustrates the velocity contour of stagnation geometry with 2 exhaust vents. The exhaust vent area to inlet area ratio was 20% and the tip of the thermocouple was at 0.01 in. from the entrance area. The divergence was detected at inlet velocity of 160 m/s.

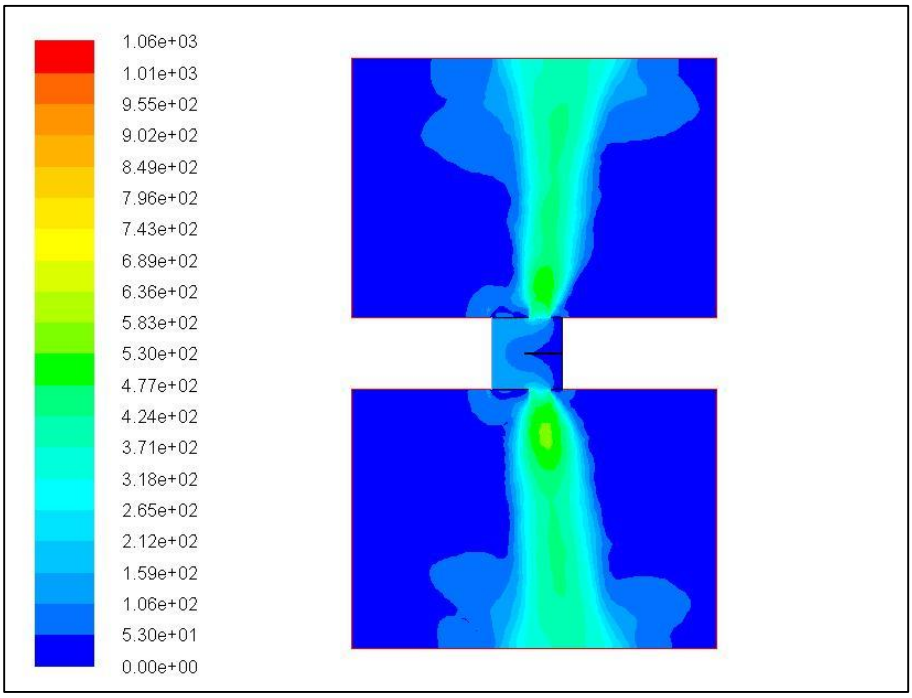

Figure 3.2: Velocity contour for the stagnation tube geometry with exhaust to entrance area ratio of 20%

Figure 3.3 shows the velocity contour of stagnation geometry with 2 exhaust vents with the exhaust vent area to inlet area ratio of 20%. The tip of the thermocouple was at 0.9 in. from the entrance area. The divergence was detected at inlet velocity of 180m/s. Although, both the geometries had different locations of exhaust vents, velocity at which the divergence was detected is same for both the cases. Other geometries with area ratio of 20% were also tested. The location of the thermocouple from the stagnation tube entrance was altered for other geometries. The velocity at which the temperature divergence occurred remained around 160 m/s.

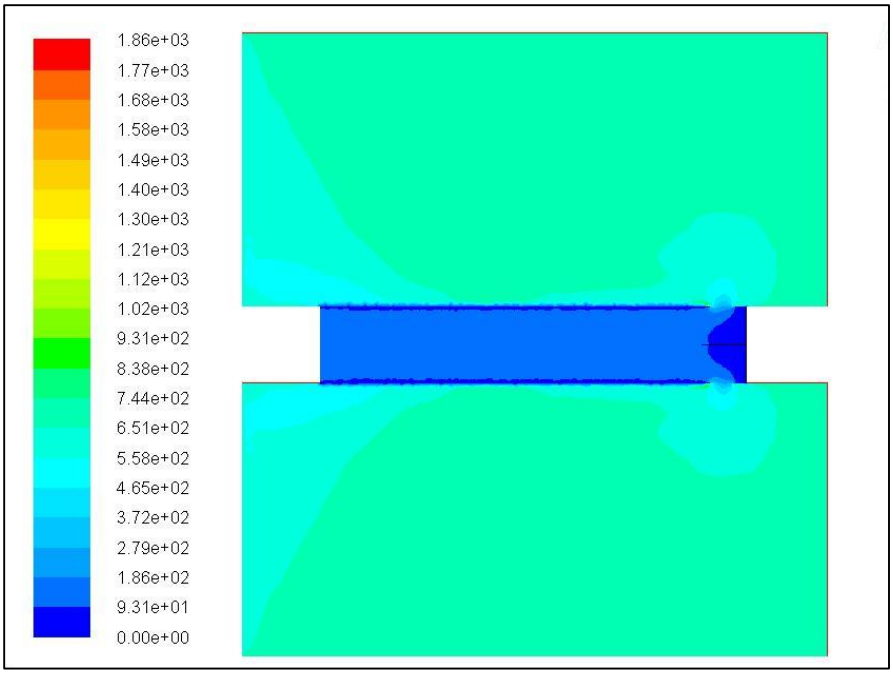

Figure 3.3: Velocity contour for the stagnation tube geometry with exhaust to entrance area ratio of 20%

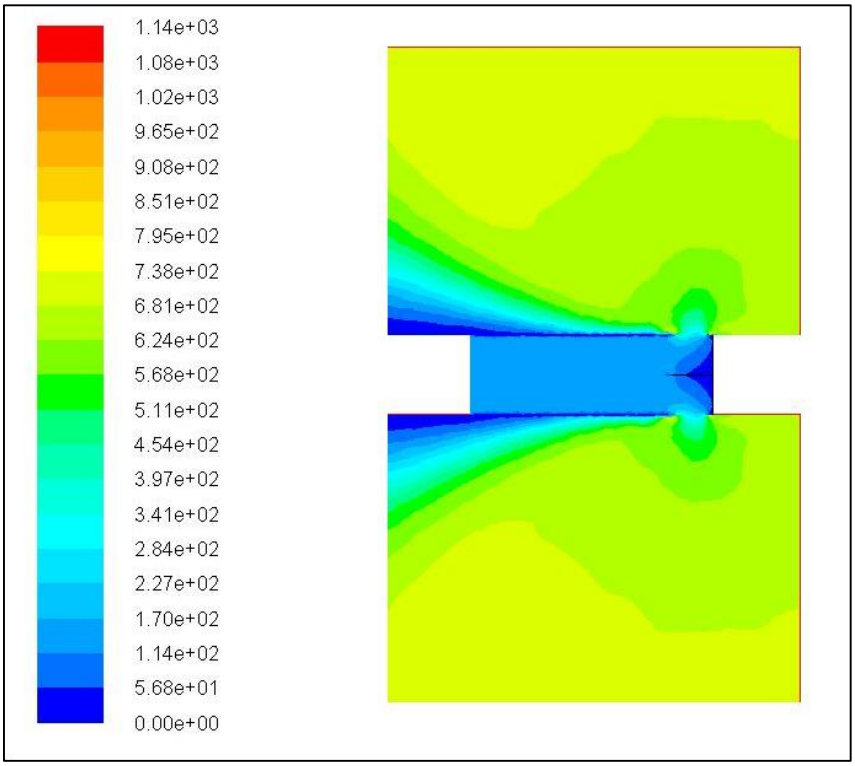

Figure 3.4: Velocity contour for the stagnation tube geometry with exhaust to entrance area ratio of 30%

Figure 3.4 illustrates the velocity contour of stagnation geometry with the exhaust vent area to inlet area ratio of 30%. The tip of the thermocouple was at 0.4 in. from the entrance area. The divergence was detected at the inlet velocity of 220m/s. It could be hypothesized that the location of the thermocouple from the entrance area does not affect the value of input velocity for which divergence occurred. Figure 3.5 illustrates the velocity contour of stagnation geometry with the exhaust vent area to inlet area ratio of 40%. The tip of the thermocouple was at 0.4 in. from the entrance area. The divergence was detected at the inlet velocity of 180m/s.

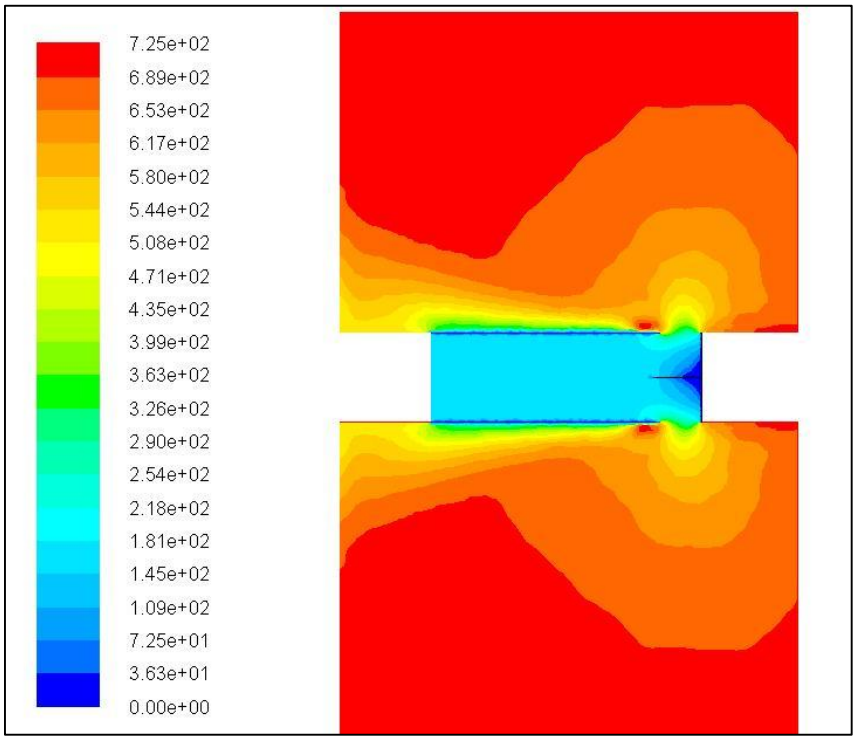

Figure 3.5: Velocity contour for the stagnation tube geometry with exhaust to entrance area ratio of 40%

Hence, the use of computational tools to decide upon the stagnation tube design was not successful and failed to provide a clear directive. The velocity at which divergence occurred was selected as a guideline for selecting the stagnation tube design. Therefore, the stagnation tube with exhaust area to inlet area ratio of 30% was selected as a final design for stagnation tube.

Chapter 4

Results and Analysis

This chapter discusses the results from the calibration as well as measurement experiments. The data acquisition system, as described in chapter 1, was used to amass data from the calibration experiments as well as measurement experiments. MATLAB and Microsoft Excel were used to process the collected data.

4.1 – Thermocouple Calibration Experiment

The calibration experiments to calculate time constant of the type E thermocouple was carried out by application of the step temperature change. Calibration experiments were first performed with AWG 20 and AWG 24 thermocouples. The starting point of the step temperature change was made the new origin. All the Figures depicted are offset by room temperature.

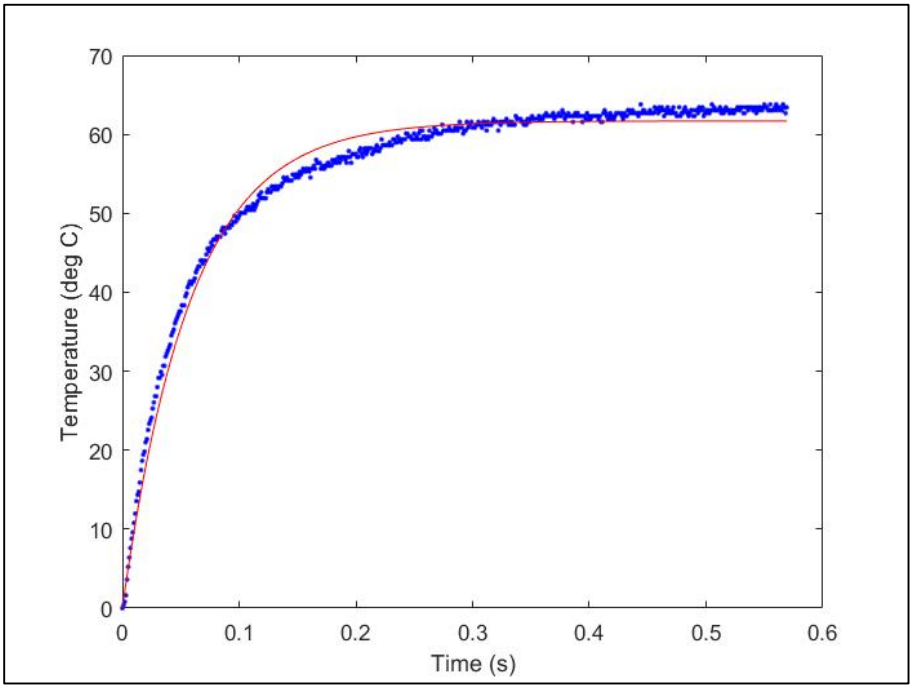

Figure 4.1: Exponential fit (Red line) applied to AWG 20 data (Blue points)

This was done to easily apply exponential curve fit to the available temperature. MATLAB was used for applying the curve fit. Figure 4.1 depicts the exponential fit applied to response of one of the AWG 20 thermocouples. Hot water was used to apply step temperature change. The steady state temperature reached was 84.3 ^{0}C when the room temperature measured was 21.9 ^{0}C and the time constant calculated was 0.085 s with an R^2 value of 0.984. The sampling rate was 1000 samples per second.

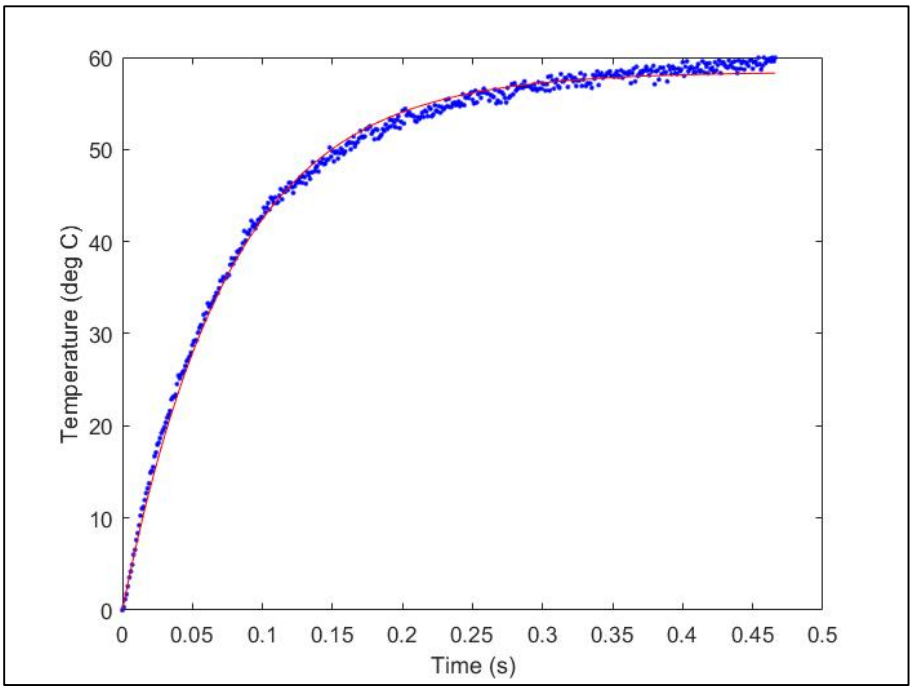

Figure 4.2: Exponential fit (Red line) applied to AWG 20 data (Blue points)

Figure 4.2 depicts the response of another AWG 20 thermocouple. In this case as well, hot water was used as a means to apply a step temperature change. The steady-state temperature reached was 82.15 ^{0}C when the measured room temperature was 21.3 ^{0}C and the time constant calculated was 0.072 s with an R^2 value of 0.9998. The sampling rate was 1000 samples per second. AWG 24 thermocouple was also calibrated by exposing it to hot water. As shown in Figure 4.3, the AWG 24 thermocouple reached the steady state temperature of 84.78 ^{0}C when the room temperature was 20.8 ^{0}C and the calibrated time constant was 0.069 s with an R^2 value of 0.9985.

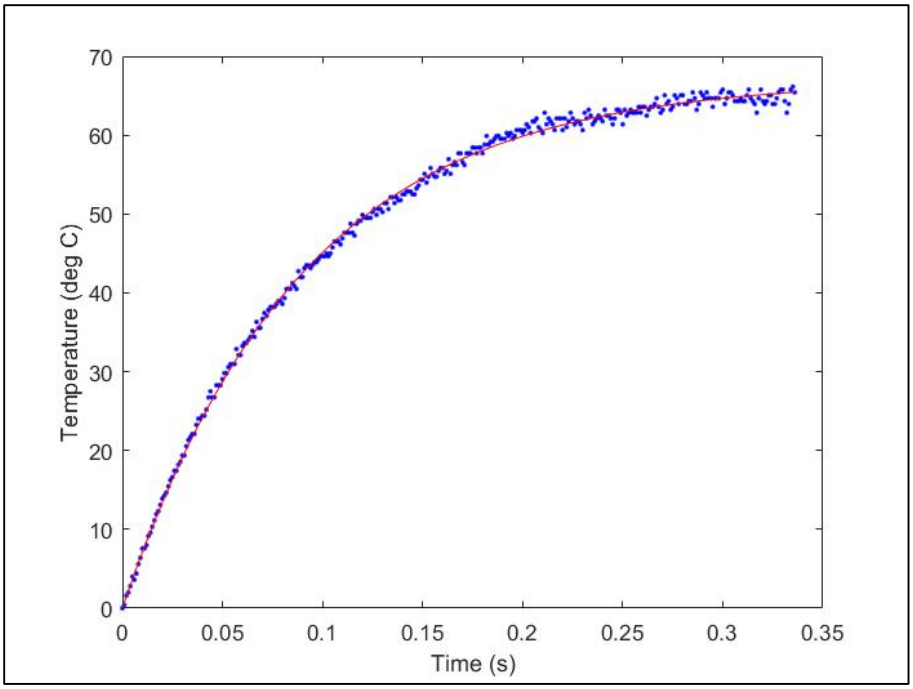

Figure 4.3: Exponential fit (Red line) applied to AWG 24 data (Blue points).

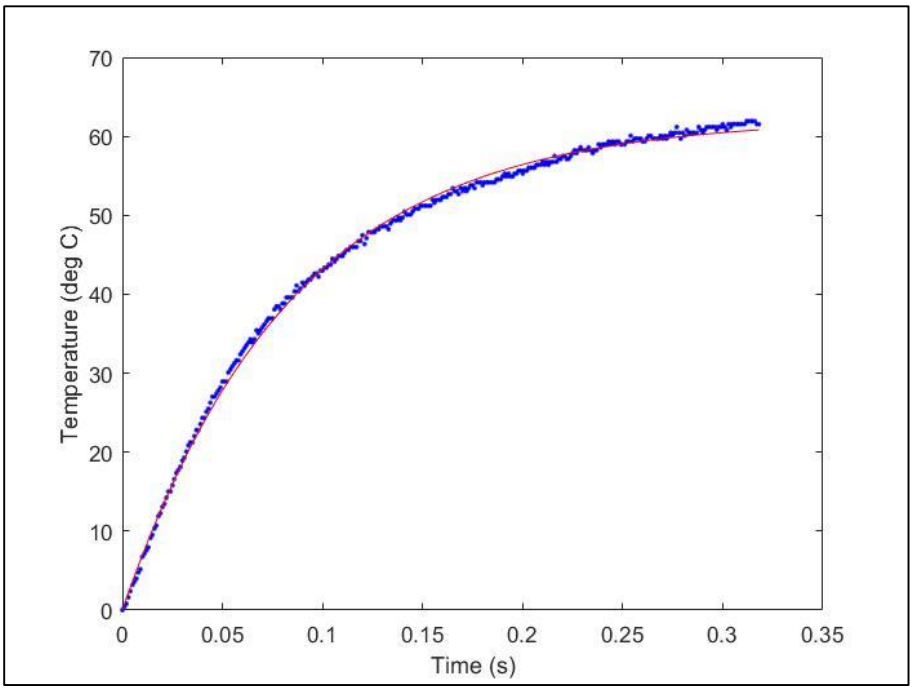

Figure 4.4: Exponential fit (Red line) applied to AWG 24 data (Blue points)

Figure 4.4 shows another dataset of AWG24 thermocouple to the step temperature change. The steady state temperature reached was 86.37 ^{0}C when the room temperature was 21.2 ^{0}C and the time constant calibrated was 0.064 s with an R^2 value of 0.9984. The sampling rate was 1000 samples per second.

The thermocouple time constant was found to be varying depending upon the number of points which were under consideration. As shown in Table 4.1 below, this variation in the number of points was achieved by altering the length of curve for which the exponential fit was applied.

Table 4.1: Time window variation for AWG 20 data

TC AWG 20 -1 Dataset1				
Sr. No	R^2	Time Window (s)	b	$\tau = 1/b$
1	0.9988	1.784 to 1.85	18.11	0.055
2	0.9986	1.784 to 1.9	15.03	0.067
3	0.9988	1.784 to 1.95	15.02	0.067
4	0.9986	1.784 to 2.0	14.56	0.069
5	0.9983	1.784 to 2.05	14.14	0.071
6	0.9978	1.784 to 2.10	13.81	0.072
7	0.9973	1.784 to 2.15	13.52	0.074
8	0.996	1.784 to 2.25	13.05	0.077
9	0.9941	1.784 to 2.35	12.64	0.079
10	0.9904	1.784 to 2.50	12.13	0.082

Table 4.2: Time window variation for AWG 20 data –thermocouple 2

TC AWG 20 - Different TC				
Sr. No	R^2	Time Window (s)	b	$\tau = 1/b$
1	0.9988	3.393 to 3.45	14.79	0.068
2	0.9994	3.393 to 3.50	13.8	0.072
3	0.9996	3.393 to 3.55	13.54	0.074
4	0.9996	3.393 to 3.60	13.46	0.074
5	0.9992	3.393 to 3.65	12.99	0.077
6	0.9978	3.393 to 3.70	12.38	0.081
7	0.996	3.393 to 3.75	11.8	0.085
8	0.9931	3.393 to 3.85	10.98	0.091
9	0.9911	3.393 to 3.95	10.46	0.096
10	0.99	3.393 to 4.0	10.26	0.097

Tables 4.1 and 4.2 shows the variation of the step response curve of AWG 20 thermocouple by varying the time window under consideration. The time constant of AWG 20 thermocouple in Table 4.1 diverged between 0.055 s and 0.082 s whereas in Table 4.2, the time constant diverged between 0.068 s and 0.097 s.

Table 4.3: Time window variation for AWG 20 data –thermocouple 3

TC AWG 20 - Different TC - Dataset 2				
Sr. No	R^2	Time Window (s)	b	$\tau = 1/b$
1	0.9993	2.079 to 2.10	26.41	0.038
2	0.999	2.079 to 2.15	19.42	0.051
3	0.9992	2.079 to 2.20	18.58	0.054
4	0.9986	2.079 to 2.25	17.34	0.058
5	0.998	2.079 to 2.30	16.53	0.060
6	0.9975	2.079 to 2.35	15.97	0.063
7	0.9973	2.079 to 2.40	15.7	0.064
8	0.9954	2.079 to 2.5	15.03	0.067
9	0.9837	2.079 to 2.75	13.48	0.074
10	0.9776	2.079 to 3	12.75	0.078

As shown in Table 4.3, the exponential fit was applied to another dataset obtained by step temperature change applied to AWG 20 thermocouple. The time constant of the AWG 20 thermocouple varied between 0.038 s and 0.078 s.

Table 4.4: Time window variation for AWG 24 data –thermocouple 2

TC AWG 24 -1 Dataset 2				
Sr. No	R^2	Time Window (s)	b	$\tau = 1/b$
1	0.9982	3.024 to 3.06	41.54	0.024
2	0.9916	3.024 to 3.11	16.8	0.060
3	0.9959	3.024 to 3.16	15.98	0.063
4	0.9971	3.024 to 3.21	16.15	0.062
5	0.9977	3.024 to 3.26	16.08	0.062
6	0.9979	3.024 to 3.31	15.99	0.063
7	0.9978	3.024 to 3.4	15.74	0.064
8	0.9959	3.024 to 3.7	15.04	0.066
9	0.9944	3.024 to 3.9	14.77	0.068
10	0.9939	3.024 to 4	14.67	0.068

Table 4.5: Time window variation for AWG 24 dataset2

TC AWG 24 -1 Dataset 2				
Sr. No	R^2	Time Window (s)	b	$\tau = 1/b$
1	0.9972	1.378 to 1.45	29.44	0.034
2	0.9935	1.378 to 1.5	21.41	0.047
3	0.9918	1.378 to 1.55	18.37	0.054
4	0.9916	1.378 to 1.6	16.94	0.059
5	0.9913	1.378 to 1.65	16.07	0.062
6	0.9912	1.378 to 1.7	15.53	0.064
7	0.9909	1.378 to 1.75	15.15	0.066
8	0.9897	1.378 to 1.85	14.54	0.069
9	0.9889	1.378 to 1.95	14.14	0.071
10	0.9887	1.378 to 2	14.06	0.071

Tables 4.4 and 4.5 show the variation of the step response curve of AWG 24 thermocouple by altering the number of data points for which the exponential fit was applied. The time constant of the AWG 24 thermocouple in Table 4.4 varied between 0.024 s and 0.068 s whereas for the data shown in Table 4.5, the time constant varied between 0.034 s and 0.071 s.

A negative step temperature change was applied to the thermocouples with the help of ice cold water. As explained in the methodology section of chapter 1, the procedure for the negative step input was same. An exponential fit was applied to the varying length of thermocouple step response which is depicted in the Table 4.6 as follows:

Table 4.6: Time window variation for AWG 20 dataset2

TC AWG 20 -1 Dataset 2				
Sr. No	R^2	Time Window (s)	b	$\tau = 1/b$
1	0.9749	1.225 to 1.4	10.12	0.099
2	0.9853	1.225 to 1.6	8.474	0.118
3	0.9803	1.225 to 1.8	6.871	0.146
4	0.9744	1.225 to 2.0	5.857	0.171
5	0.9741	1.225 to 2.15	5.534	0.181
6	0.9772	1.225 to 2.3	5.288	0.189

Table 4.7: Time window variation for AWG 20 dataset1

TC AWG 20 -1 Dataset1				
Sr. No	R^2	Time Window (s)	b	$\tau = 1/b$
1	0.9916	0.907 to 1.2	10.64	0.094
2	0.9816	0.907 to 1.4	8.006	0.125
3	0.98	0.907 to 1.6	7.1	0.141
4	0.9778	0.907 to 1.8	6.612	0.151
5	0.9766	0.907 to 1.9	6.428	0.156
6	0.9748	0.907 to 2.06	6.207	0.161

Table 4.8: Time window variation for AWG 20 dataset2

TC AWG 20-2 -1 Dataset2				
Sr. No	R^2	Time Window (s)	b	$\tau = 1/b$
1	0.9923	0.873 to 1	16.12	0.062
2	0.9905	0.873 to 1.1	12.72	0.079
3	0.9851	0.873 to 1.2	10.29	0.097
4	0.9865	0.873 to 1.4	9.185	0.109
5	0.9871	0.873 to 1.6	8.92	0.112
6	0.9863	0.873 to 1.8	8.735	0.114

Tables 4.6 and 4.7 show the variation of the step response curve of AWG 20 thermocouple by changing the number of data points for which the exponential fit was applied. The time constant of AWG 20 thermocouple in Table 4.6 ranged between 0.099 and 0.189 s whereas in Table 4.7, the time constant ranged between 0.094 and 0.161 s. Another set of data obtained from the step response of the AWG 20 thermocouple was analyzed and the results displayed in Table 4.8. The time constant for this dataset ranged between 0.062 and 0.114 s.

The AWG 24 thermocouple was also calibrated by using cold water as step input. Tables 4.9 and 4.10 show the changes of the step response curve of AWG 24 thermocouple by modifying the time window under consideration. The time constant of AWG 24 thermocouple in Table 4.9 ranges between 0.118 and 0.129 s whereas in Table 4.10, the time constant diverged between 0.093 and 0.104 s. Table 4.10 shows the time constant variation for another dataset AWG 24 where the time constant varied between 0.089 and 0.120 s.

Table 4.9: Time window variation for AWG 24 dataset1

TC AWG 24 -1 Dataset1				
Sr. No	R^2	Time Window (s)	b	$\tau = 1/b$
1	0.9949	1.257 to 1.6	8.459	0.118
2	0.995	1.257 to 1.7	8.26	0.121
3	0.9949	1.257 to 1.8	8.095	0.124
4	0.9942	1.257 to 1.9	7.929	0.126
5	0.9936	1.257 to 2.0	7.778	0.129

Table 4.10: Time window variation for AWG 24 dataset2

TC AWG 24 -1 Dataset2				
Sr. No	R^2	Time Window (s)	b	$\tau = 1/b$
1	0.9947	1.376 to 1.6	10.74	0.093
2	0.9957	1.376 to 1.7	10.23	0.098
3	0.9951	1.376 to 1.8	10.09	0.099
4	0.9943	1.376 to 1.9	9.804	0.102
5	0.9939	1.376 to 2.0	9.653	0.104

Table 4.11: Time window variation for AWG 24 dataset2

TC AWG 24 -1 Dataset3				
Sr. No	R^2	Time Window (s)	b	$\tau = 1/b$
1	0.9882	1.477 to 1.63	11.21	0.089
2	0.9894	1.477 to 1.73	10.33	0.097
3	0.99	1.477 to 1.83	9.217	0.108
4	0.9897	1.477 to 1.93	8.624	0.116
5	0.9899	1.477 to 2.03	8.359	0.120

Another set of data obtained from the step response of AWG 20 thermocouple was analyzed and the reduced data obtained are shown in Table 4.8. The time constant for this dataset varied between 0.062 and 0.114 s. Hence, by both the methods, it can be shown that time constant of AWG 20 is larger than that of AWG 24.

AWG 50 thermocouple is the tiniest and supposedly the fastest thermocouple of all the thermocouples which were used for the stagnation temperature measurement. The wire diameter

of the AWG 50 thermocouple is 0.001 in. and hence the thermocouple required special care while handling. As explained in chapter 1, the error fraction approach was implemented to find out the time constant and verify it with other time constant found out by applying exponential fit.

Figure 4.5 depicts the exponential fit applied to the step response of the AWG 50 thermocouple. The time constant obtained was 0.0032 s with an R^2 value of 0.8107. Due to the fragile nature of the thermocouple, the data obtained was influenced by the noise and fluctuates around the actual thermocouple response. Hence, the R^2 value is low.

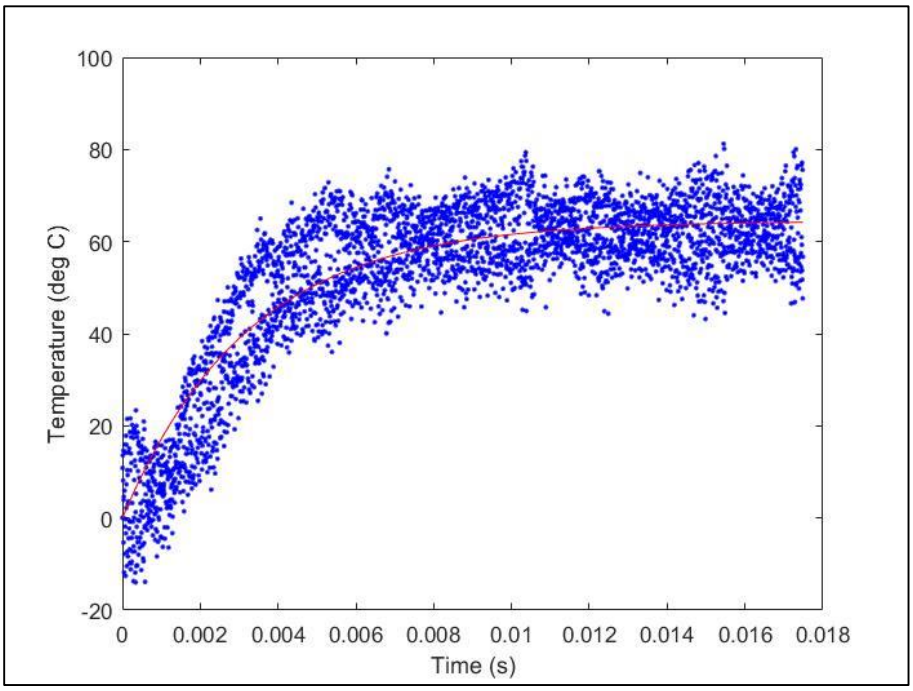

Figure 4.5: Exponential fit (Red line) applied to AWG 50 data (Blue points)

Figure 4.6 shows the exponential fit applied to the error fraction of the step response of AWG 50 thermocouple. The time constant was found to be 0.0023 s with an R^2 value of 0.7962. Both the time constants were found to be in close proximity of each other. In order to mitigate the influence of noise on the step response, the moving average method was also implemented. The points under consideration in moving average method were 5, 15 or 25 points.

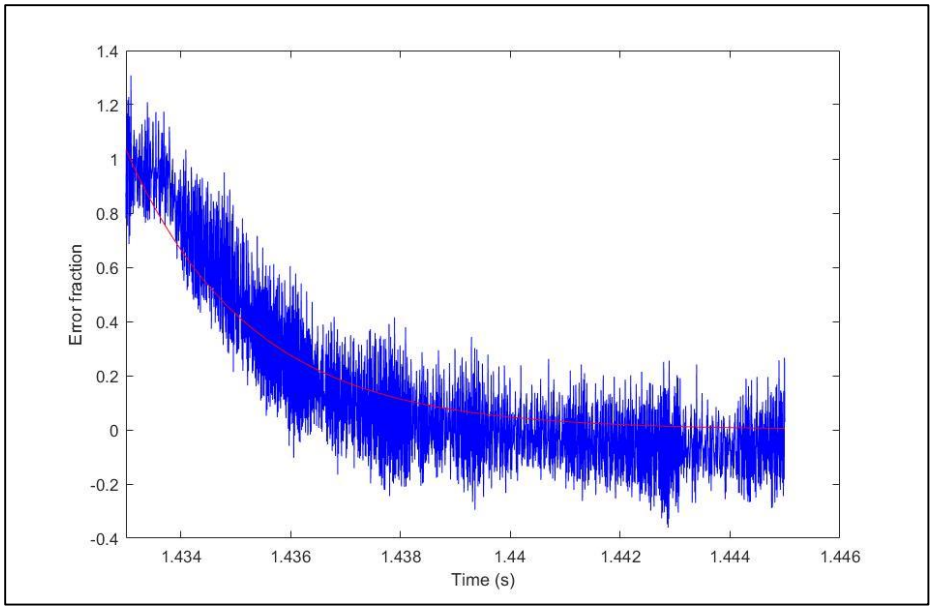

Figure 4.6: Error fraction- Exponential fit (Red line) applied to AWG 50 data (Blue points)

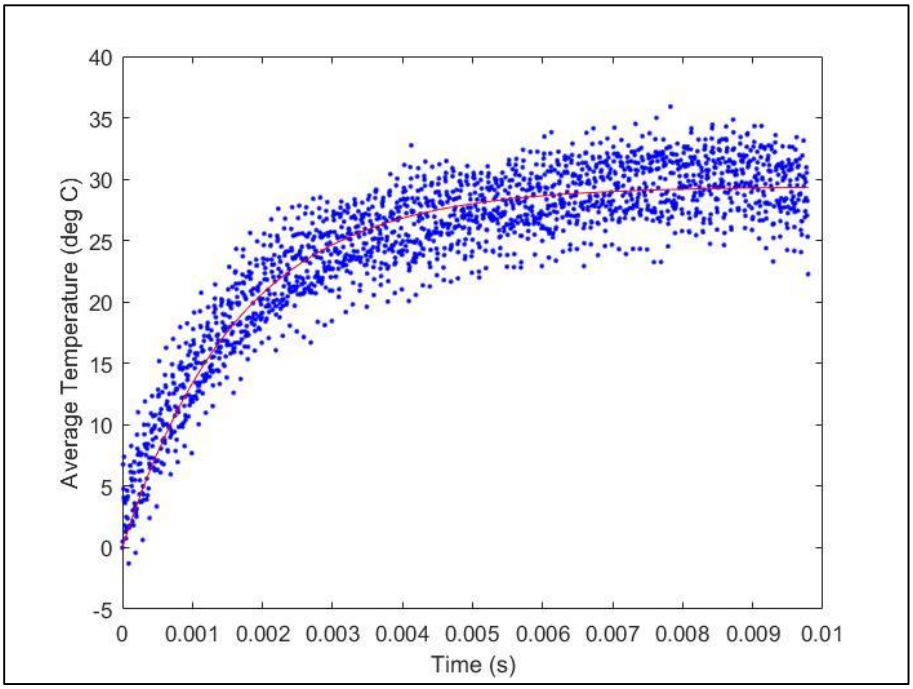

Figure 4.7: Moving average 5: Exponential fit (Red line) applied to AWG 50 data (Blue points)

Moving averages of temperature values were taken and the values were plotted against time. For each point, moving average of either 5, 15 or 25 number of points was taken. Figure 4.6 shows the case where moving average of 5 points was taken. The time constant obtained was 0.00198 s and the R^2 value was 0.9682. For the case with moving average of 15 points, time constant found was 0.002 s and the R^2 value was 0.9934. The exponential fit applied to this case is illustrated in Figure 4.7.

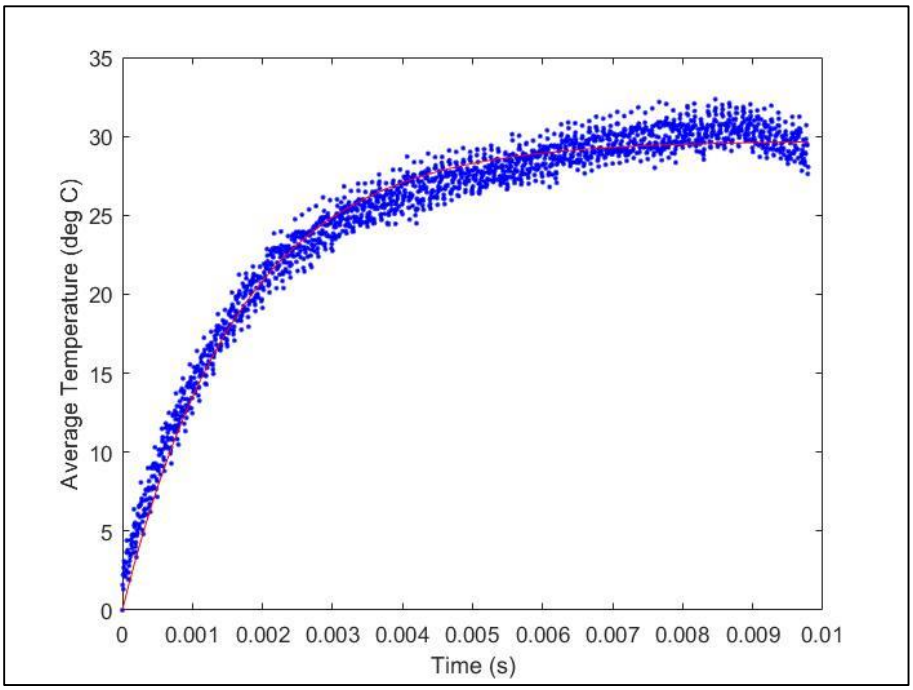

Figure 4.8: Moving average 15: Exponential fit (Red line) applied to AWG 50 data (Blue points)

Figure 4.8 shows the case where a moving average of 15 points was taken. The time constant obtained for the case was 0.0021 s and the R^2 value was 0.9948. The time constant does not vary much for all three cases.

The use of cold water to apply a step temperature change was found to be ineffective in the case of AWG 50 thermocouples. The sensitive nature of thermocouple causes the temperature to fluctuate within the range. The applied step response is smaller in magnitude when cold water is used as the temperature drop is from room temperature to 0 ^{0}C. This along with the fluctuating output makes it hard to distinguish the step response output of the thermocouple.

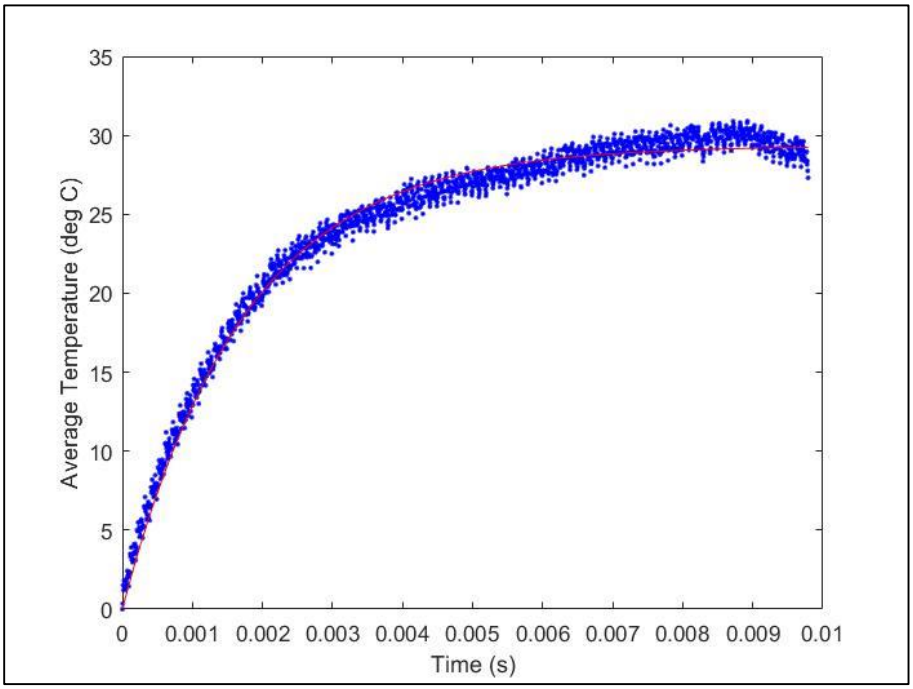

Figure 4.9: Moving average 25: Exponential fit (Red line) applied to AWG 50 data (Blue points)

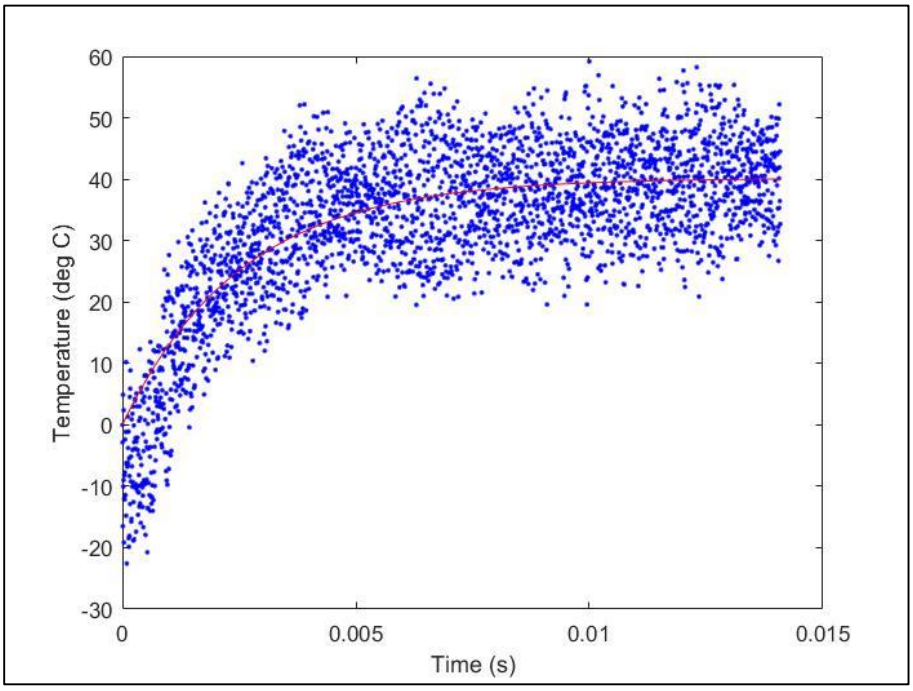

Figure 4.10: Exponential fit (Red line) applied to AWG 50 data (Blue points)

Figure 4.9 shows another plot of step response of AWG 50 thermocouple data wherein the exponential fit was applied to it. The time constant was found to be 0.0019 s and the R^2 value was 0.6676. Figure 4.10 shows the result of exponential fit applied to the error fraction of the step response. The time constant for this approach was found out to be 0.003 s and the R^2 value was 0.8029.

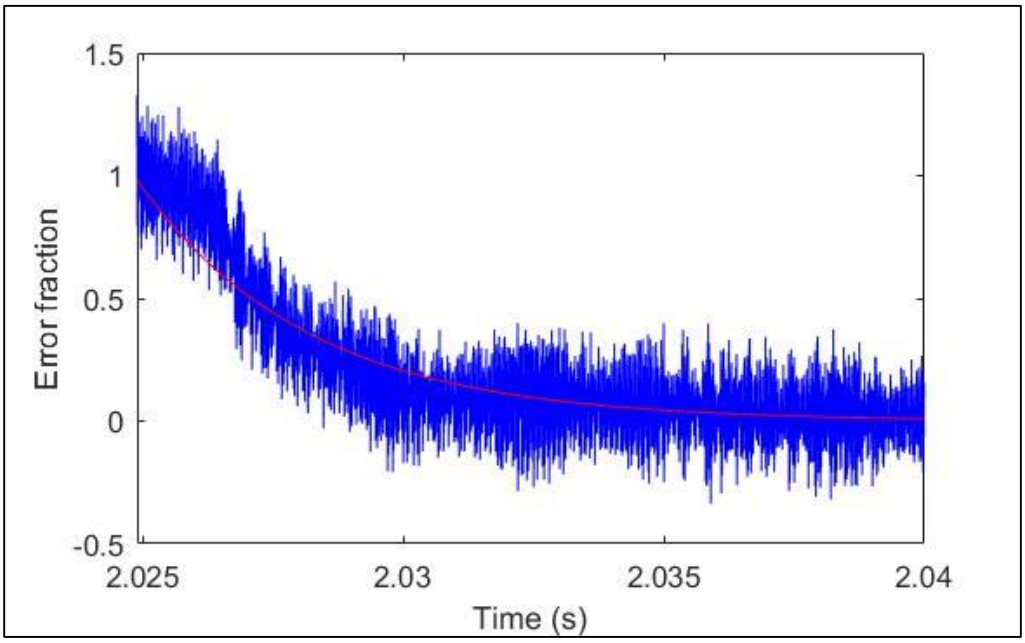

Figure 4.11: Error fraction approach: Exponential fit (Red line) applied to AWG 50 data (Blue points)

As discussed before, the moving average method was adopted to minimize the effect of noise over the step response output. The number of points under consideration which were averaged to get values at each point were either 5, 15 or 25 points. Figure 4.11 portrays the output for the case 1 where average of points was taken at each point. The time constant calculated is 0.00199 s and the R^2 value is 0.9457. Figure 4.12 illustrates case 2 where average of 15 points was obtained at each point. The time constant found for this case is 0.002 s and the R^2 value was 0.9819.

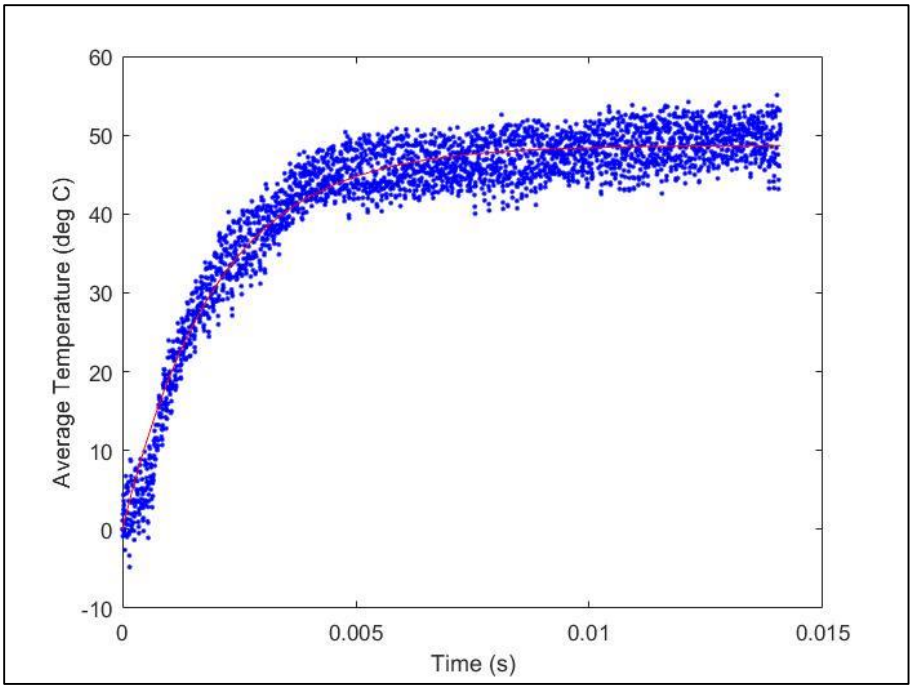

Figure 4.12: Moving average 5: Exponential fit (Red line) applied to AWG 50 data (Blue points).

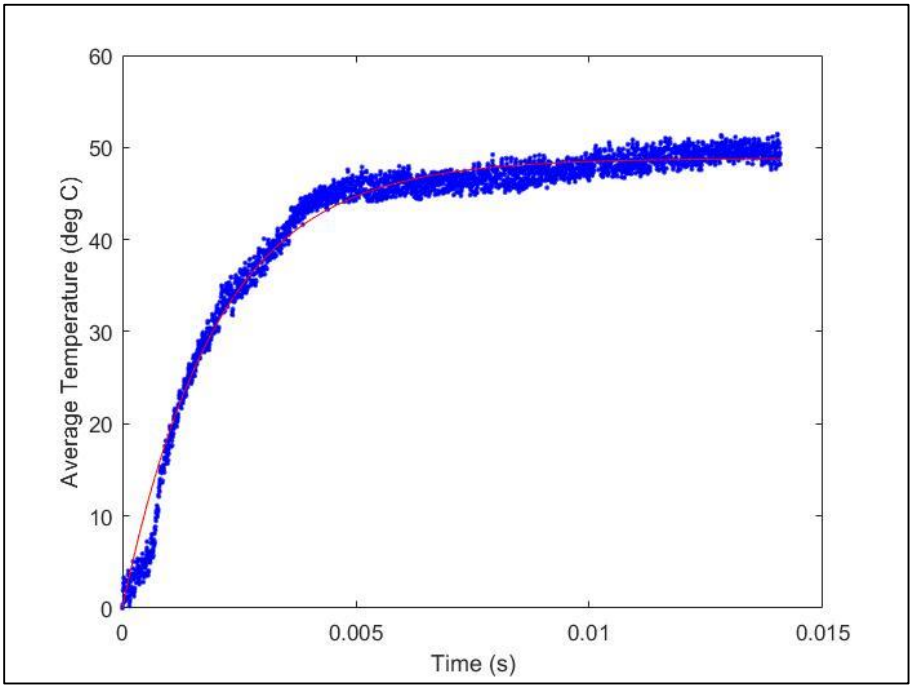

Figure 4.13: Moving average 15: Exponential fit (Red line) applied to AWG 50 data (Blue points).

Figure 4.13 depicts case 3 where average of 25 points was taken at each point. The time constant calibrated for this case was 0.002 s and the R^2 value was 0.9819. As the number of points which were averaged per point increased, the trend of R^2 values improved. This proves the hypothesis that the noise affects the data captured from thermocouple and effect of noise can be mitigated with the help of statistical means such as the moving average method.

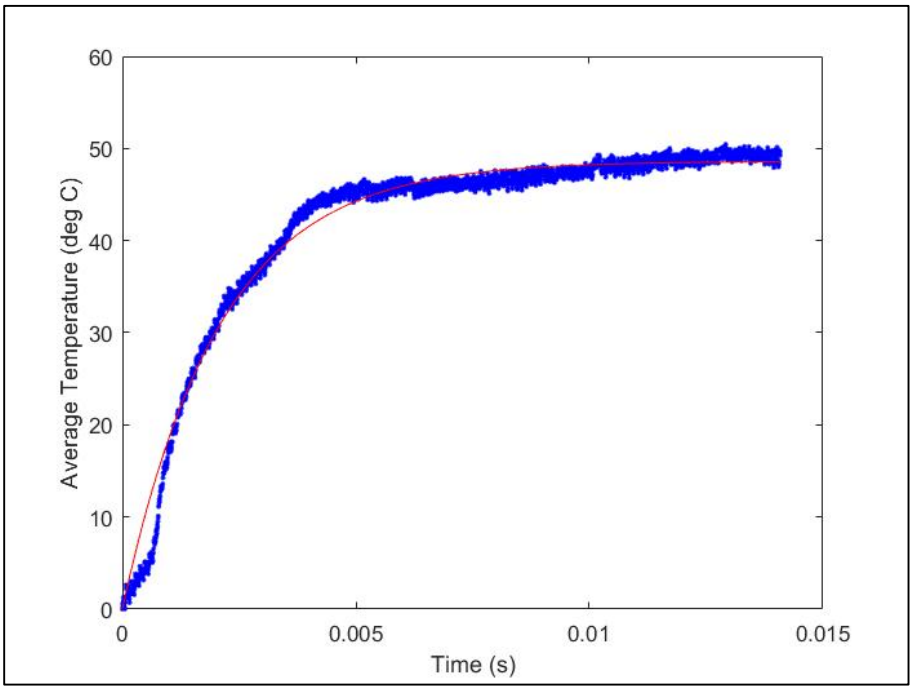

Figure 4.14: Moving average 25: Exponential fit (Red line) applied to AWG 50 data (Blue points).

4.2 – Exhaust Pressure Measurement

The exhaust pressure measurement experiment obtained pressure not only outside the detonation tube but also the pressure along the inside wall. As mentioned in chapter 1, the exhaust pressure measurement involved using the data acquisition system to capture the data from pressure transducers. The data from two pressure transducers shown in Figure 4.15, which are situated just before the tube exhaust, was collected. The wedge with pressure transducer was adjusted at different distance from the detonation tube exhaust. The pressure profiles from experiments have been illustrated in following Figures. The pressure values from the detonation tube are synonymous with the previous findings. [4]

Figures 4.14 to 4.17 depict the pressure profile from the pressure transducers which are along the detonation tube. The pressure transducers were numbered 3 and 4 with numbering starting from the closed end of the detonation tube. Figure 4.14 illustrates plot of pressure profile for transducers number 3. The pressure profile in scatter diagram format is shown in Figure 4.15. The filling fraction was 1 which means the tube was completely filled.

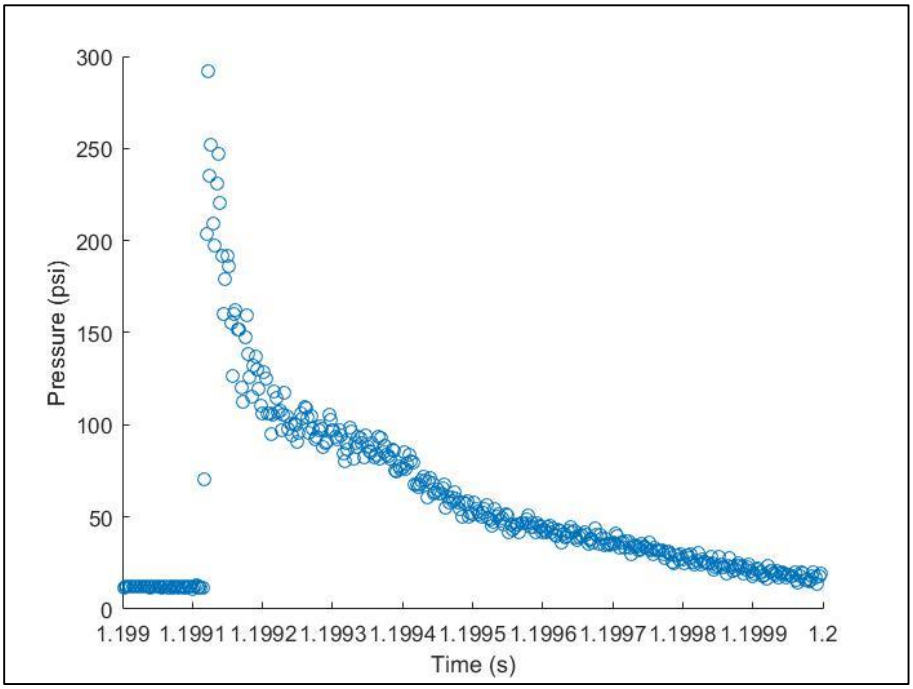

Figure 4.15: Scatter diagram of measured pressure at transducer 3

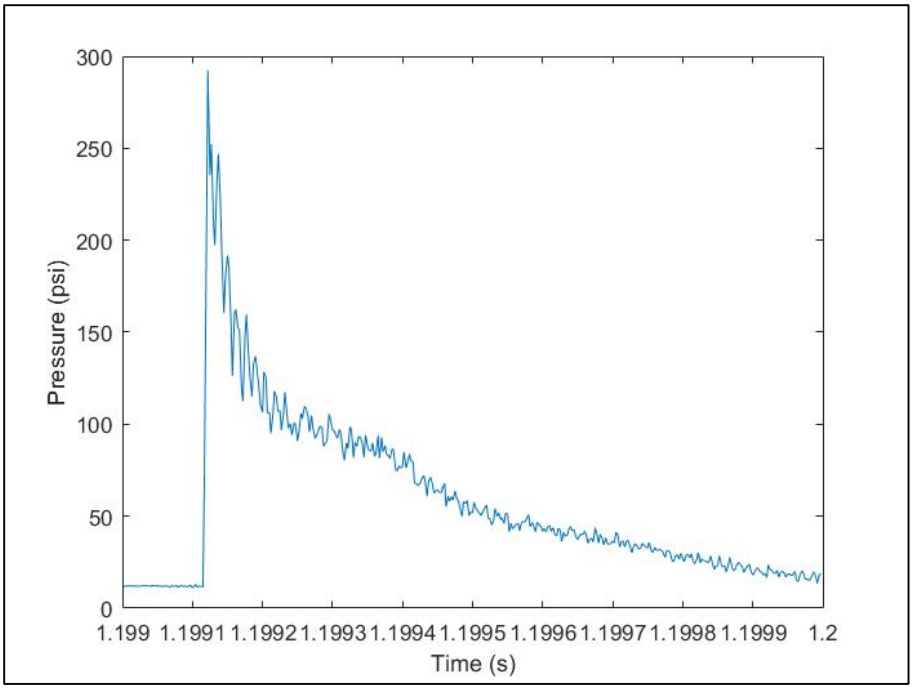

Figure 4.16: Pressure profile of measured pressure at transducer 3

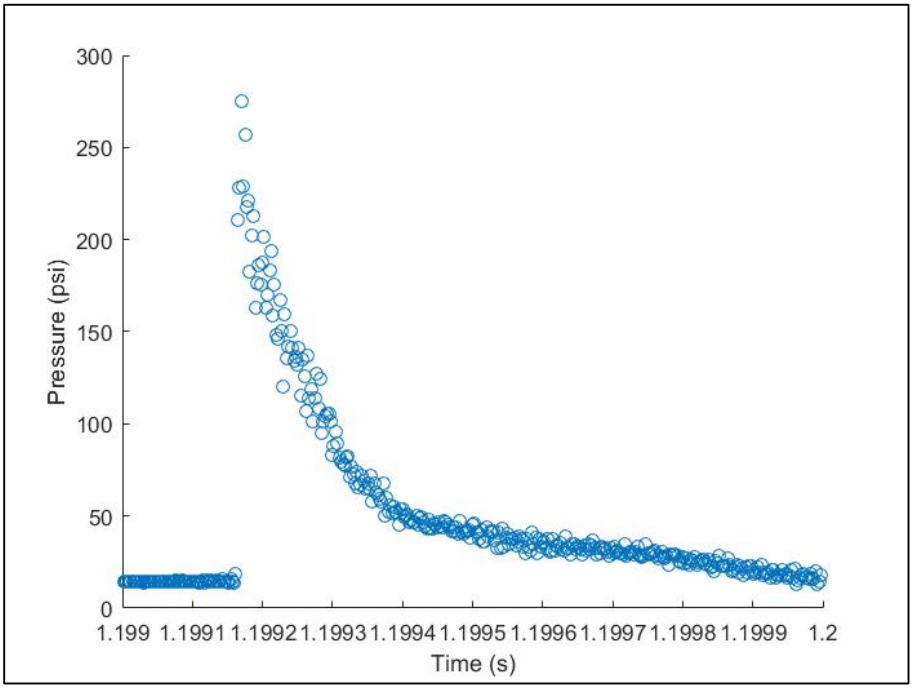

Figure 4.17: Scatter diagram of measured pressure at transducer 4

Figure 4.16 depicts the pressure profile from the pressure transducers number 4. Figure 4.17 illustrates the pressure profile of measured pressure in scatter format. The maximum pressure reached in case of transducer 3 was 295 psi whereas the maximum pressure in case of transducer 4 was 275 psi.

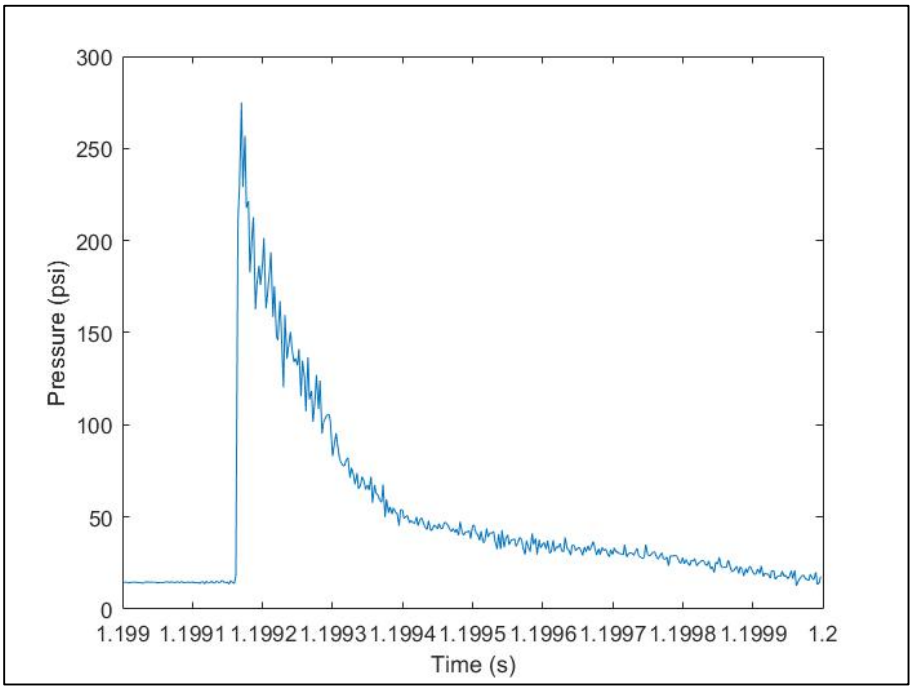

Figure 4.18: Pressure profile of measured pressure at transducer 4

Figure 4.18 illustrates the pressure profile of the exhaust pressure and Figure 4.19 shows the pressure profile of measured pressure in scatter format. The pressure transducers outside the detonation tube was at 0.27 in. from the detonation tube end. The maximum exhaust pressure reached at 0.27 in. from exhaust was 207 psi.

The velocity of the detonation wave while it was traversing through the detonation wave can be computed by using time-of-flight. The distance between the pressure transducers 3 and 4 is fixed i.e. 3.937 in. (10 cm). Also, the distance between the pressure transducer 4 and exhaust pressure measurement pressure transducer can be easily found. Hence, the detonation velocity and the wave velocity of the exited detonation wave in ambient air are 2083 and 1024 m/s. The combined pressure profiles of transducers 3 and 4 are depicted in Figure 4.20.

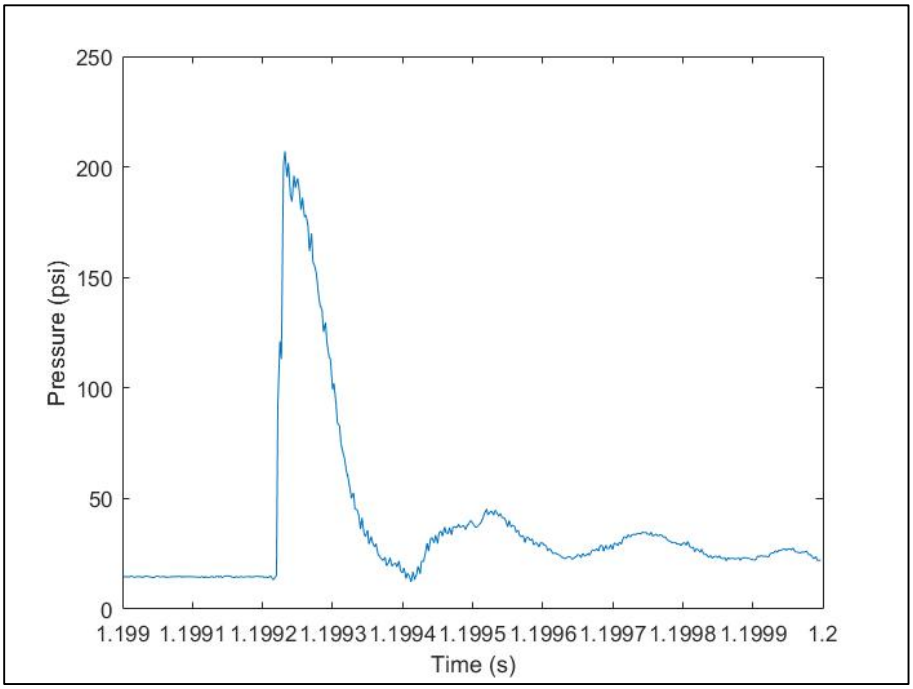

Figure 4.19: Pressure profile of exhaust pressure at 0.27 in. from detonation tube end

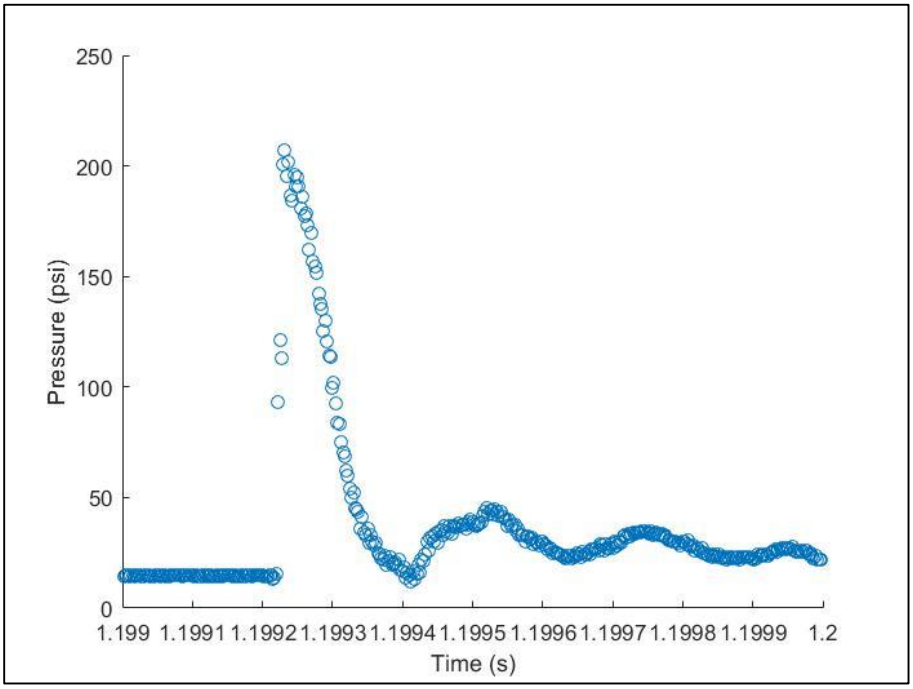

Figure 4.20: Scatter diagram of exhaust pressure at 0.27 in. from detonation tube end

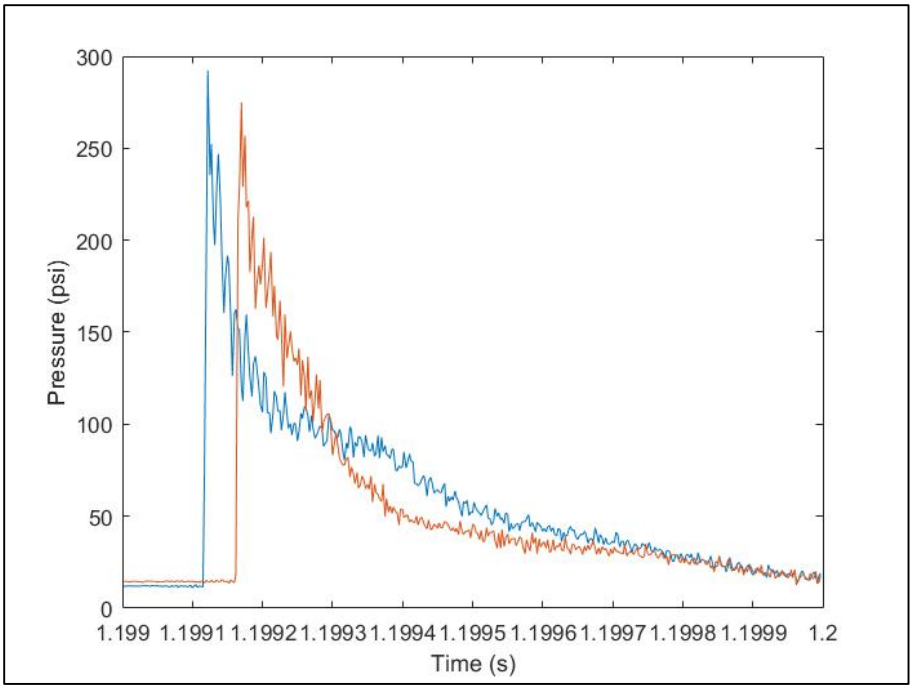

Figure 4.21: Combined pressure profile of measured pressure at transducers 3 and 4

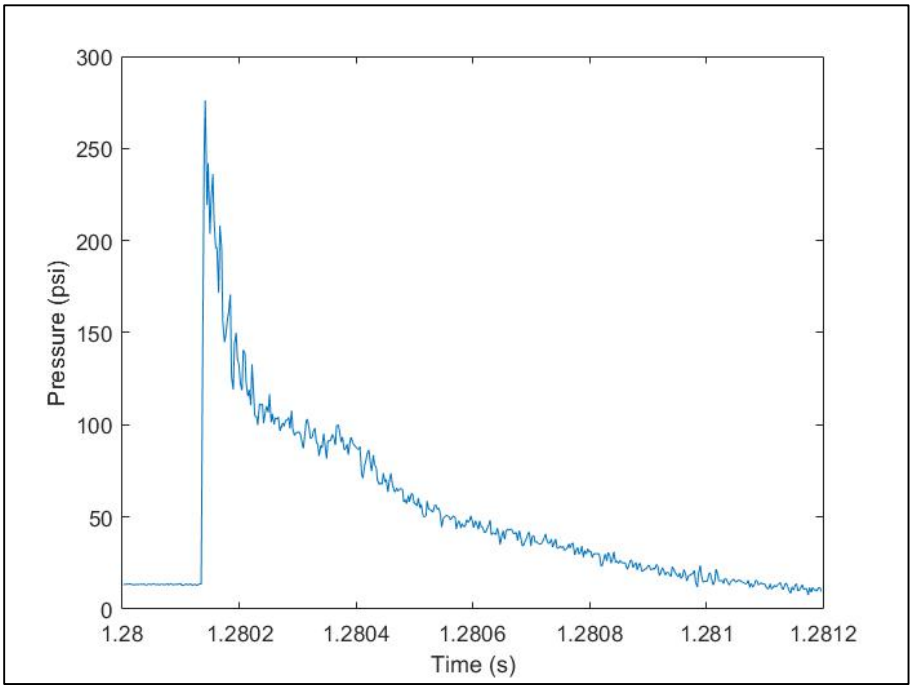

Figure 4.22: Pressure profile of measured pressure at transducer 3

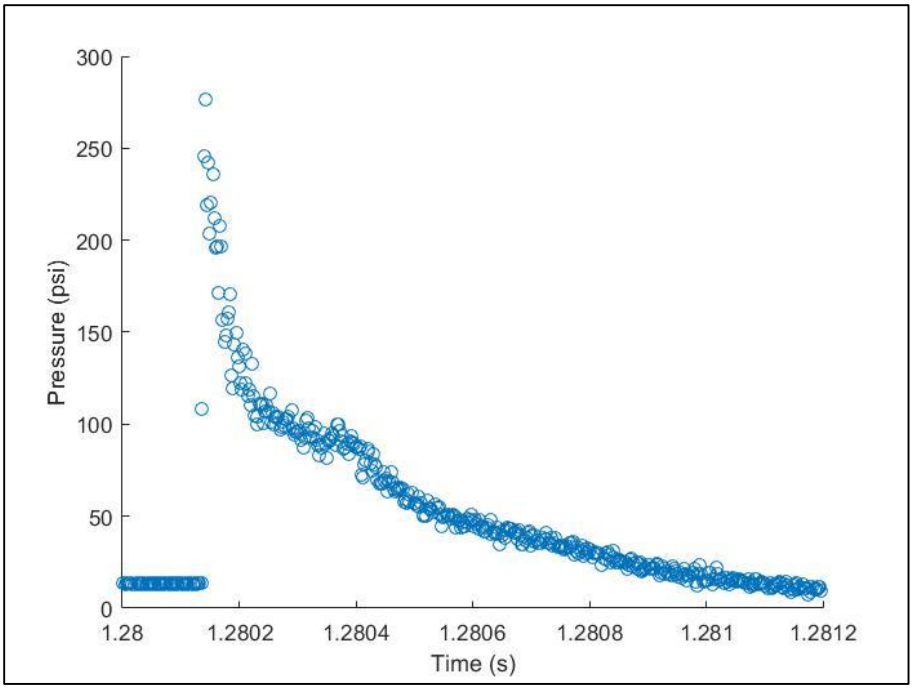

Figure 4.23: Scatter diagram of pressure profile of measured pressure at transducer 3

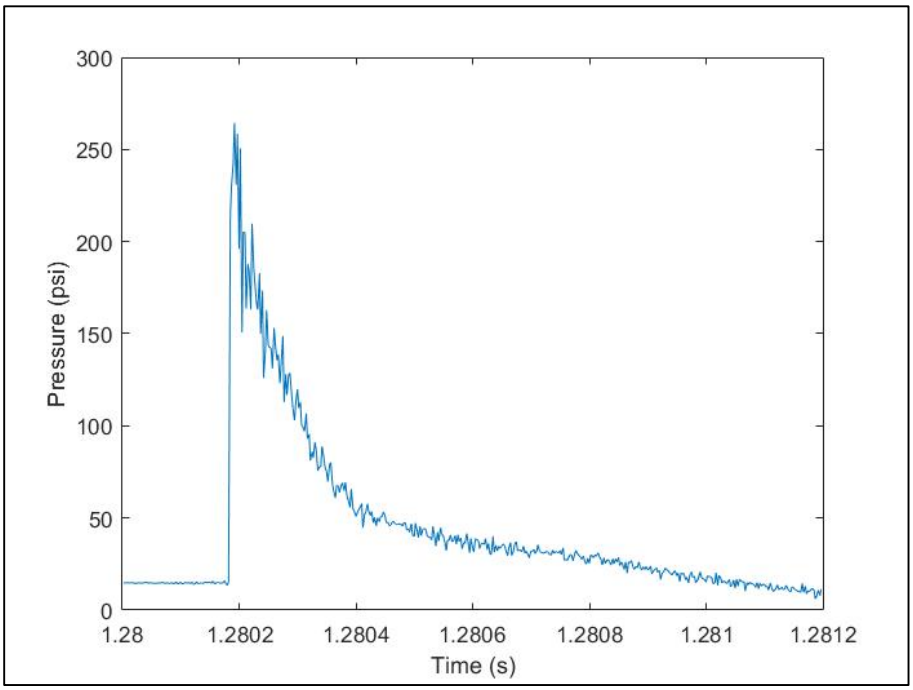

Figure 4.24: Pressure profile of measured pressure at transducer 4

Figure 4.21 depicts the pressure profile from the pressure transducers number 3. Figure 4.22 illustrates the pressure profile in scatter format. The maximum pressure reached in case of transducer 3 was 276 psi. Figure 4.23 depicts the pressure profile from the pressure transducers number 4. Figure 4.24 illustrates the pressure profile in scatter format. Maximum pressure reached in case of transducer 4 was 264 psi.

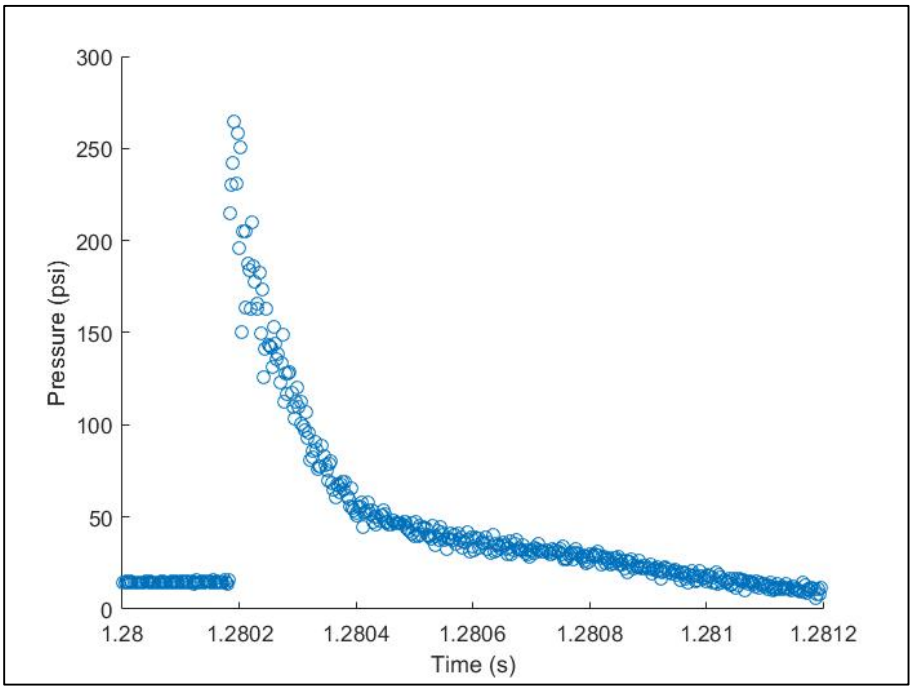

Figure 4.25: Scatter diagram of pressure profile of measured pressure at transducer 4

Figure 4.24 portrays the pressure profile of the exhaust pressure and Figure 4.25 shows the pressure profile of measured pressure in scatter format. The pressure transducer was 10 in. from the detonation tube end. The maximum exhaust pressure reached at 10 in. from exhaust was 20.147 psi. The detonation velocity and the wave velocity of the exited detonation wave in ambient air are 2000 and 518 m/s respectively. The exhaust pressure and wave velocity at 6.25 in. from the detonation tube end was also found to check whether the trend followed by exhaust pressure and exhaust velocity is linear or non-linear.

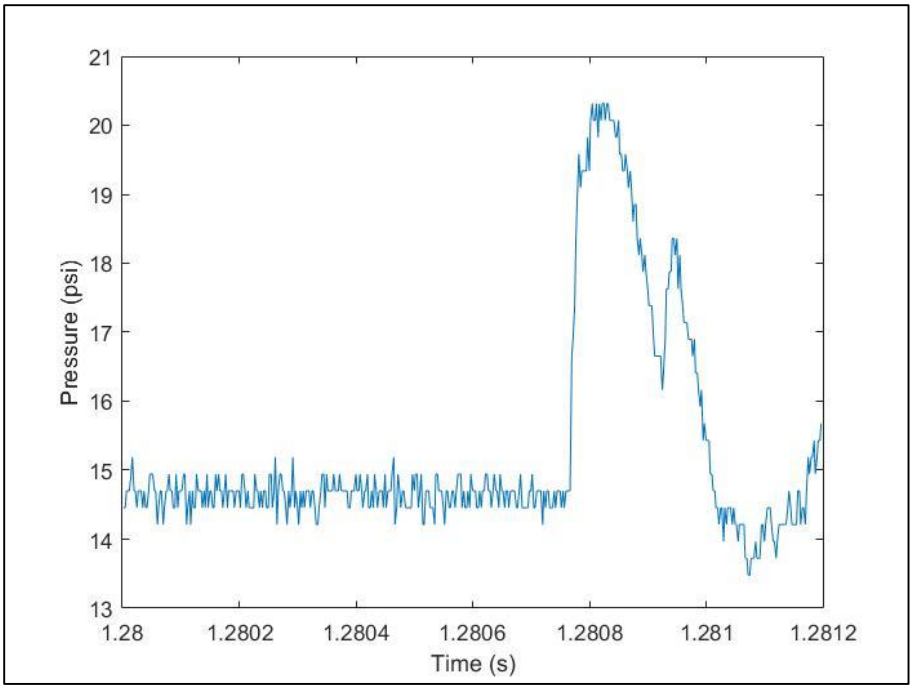

Figure 4.26: Pressure profile of exhaust pressure at 10 in. from detonation tube end

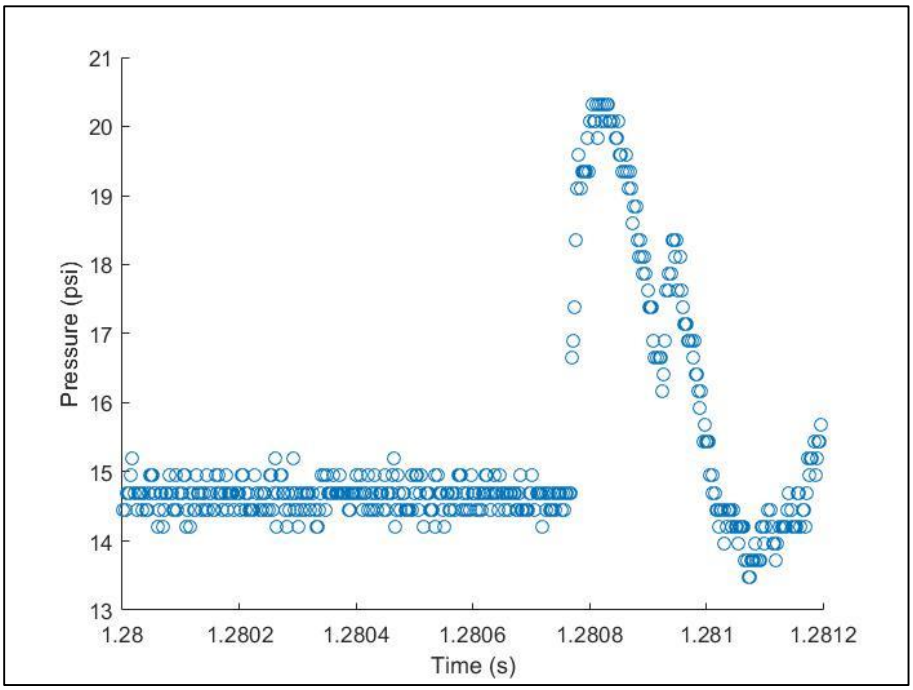

Figure 4.27: Scatter diagram of exhaust pressure at 10 in. from detonation tube end

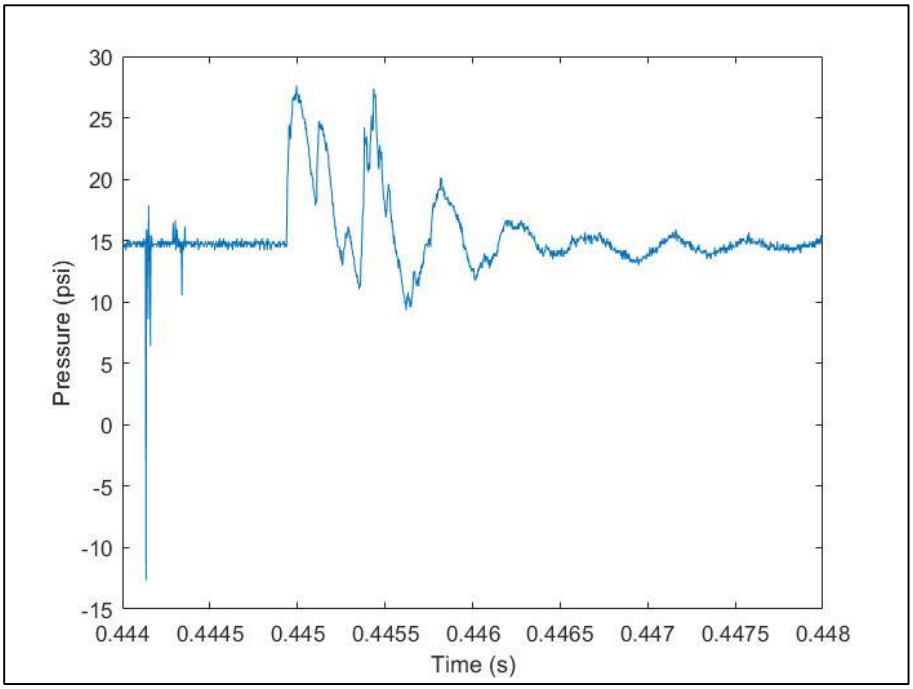

Figure 4.28: Pressure profile of exhaust pressure at 6.25 in. from detonation tube end

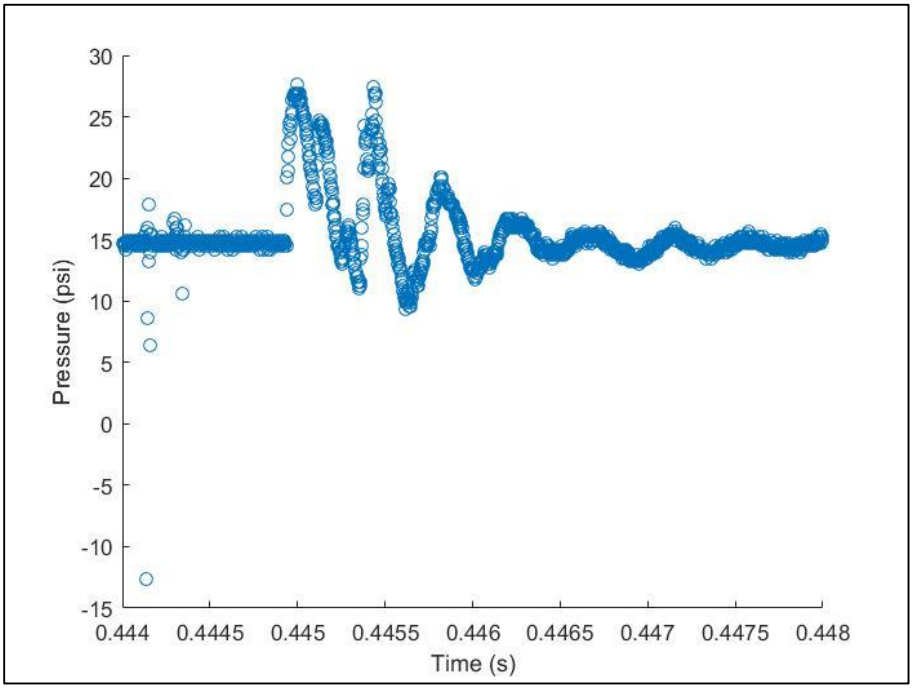

Figure 4.29: Scatter diagram of exhaust pressure at 6.25 in. from detonation tube end

Figure 4.26 portrays the pressure profile of the exhaust pressure and Figure 4.27 shows the pressure profile of measured pressure in scatter format. As mentioned above, the exhaust pressure was measured at 6.25 in. from detonation tube open end. The maximum pressure recorded at transducers 3 and 4 were 314 and 254 psi respectively. As shown in Figure 4.28 and Figure 4.29, exhaust pressure was 27.39 psi. The detonation wave velocity inside the tube and after exit from the tube were found as 2127 and 563.74 m/s respectively. Table 4.12 lists the computed wave velocity of the detonation wave when it was travelling inside as well as outside the detonation tube.

Table 4.12: Table of velocities computed by time of flight formula

			Pulse 1		Pulse2		Pulse3	
Dataset	Fuel Fraction	Distance from exhaust vent (in.)	Detonation velocity (m/s)	Wave velocity after the exhaust (m/s)	Detonation velocity (m/s)	Wave velocity after the exhaust (m/s)	Detonation velocity (m/s)	Wave velocity after the exhaust (m/s)
1	1	0.27	2083	1024	-	-	-	-
3	0.75	0.27	1428	933	-	-	-	-
4	0.75	0.27	1923	668	-	-	-	-
5	0.5	0.27	833	358			-	-
8	1	10.25	2000	517	1818	496	-	-
9	1	10.25	-	-	1667	493	-	-
11	0.75	10.25	1538	625	1538	180	1538	241
13	0.5	10.25	854	186			-	-
16	1	6.25	2128	261	1818	563	1818	256
17	1	6.25	1818	568	1923	568	-	-
18	0.75	6.25	1923	234	1538	249	-	-
19	0.75	6.25	1428	200	1587	215	1389	222
20	0.5	6.25	833	201		-	-	-
25	1	6.25	1539	447	-	-	-	-

4.3 – Exhaust Temperature Measurement

As mentioned before, type E thermocouples were used to measure the temperature at pulse detonation engine exhaust. AWG 20 and AWG 24 thermocouples were directly connected to extension wires and inserted in the stagnation tube. The measurement experiment started off with AWG 20 thermocouple as the thermocouple had lowest response time amongst the calibrated thermocouples. The filling fraction of the detonation tube was varied from 0.25 to 1 at stoichiometric air-fuel ratio. All the values were in the range of 60 to 130 ^{0}C. The temperature values observed were very low as compared to the values obtained from the normal shock relations.

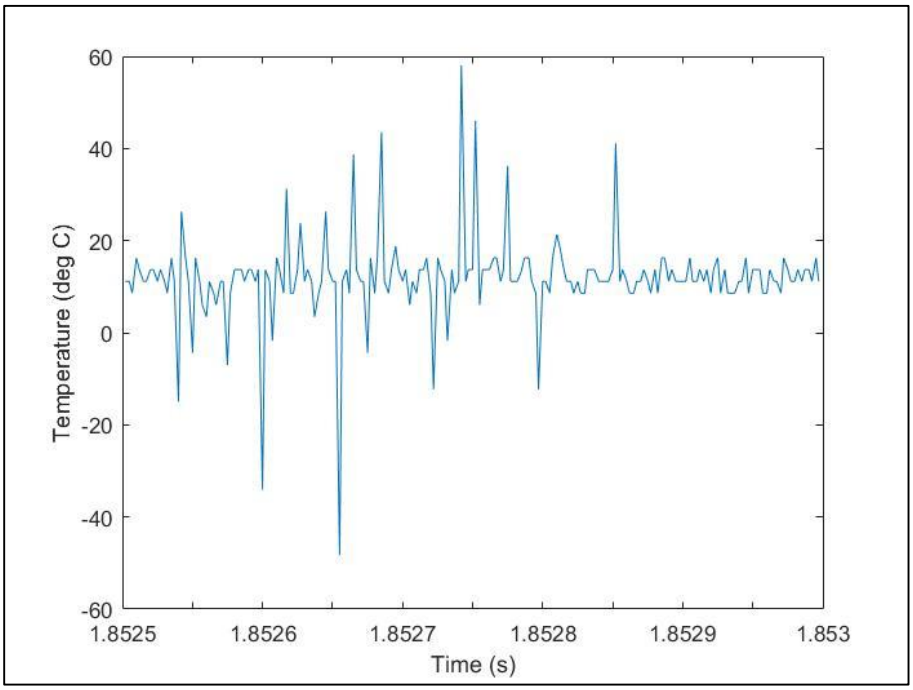

Figure 4.30: Exhaust temperature at 0.5 in. from detonation tube end measured by AWG 20 thermocouple

Figure 4.30 portrays the plot of exhaust temperature against time. The probe was situated at 0.5 in. from the detonation tube exhaust. As observed in the figure, the temperature increase does not follow the step response trend and can be found fluctuating. Figure 4.31 shows the scatter diagram of thermocouple response.

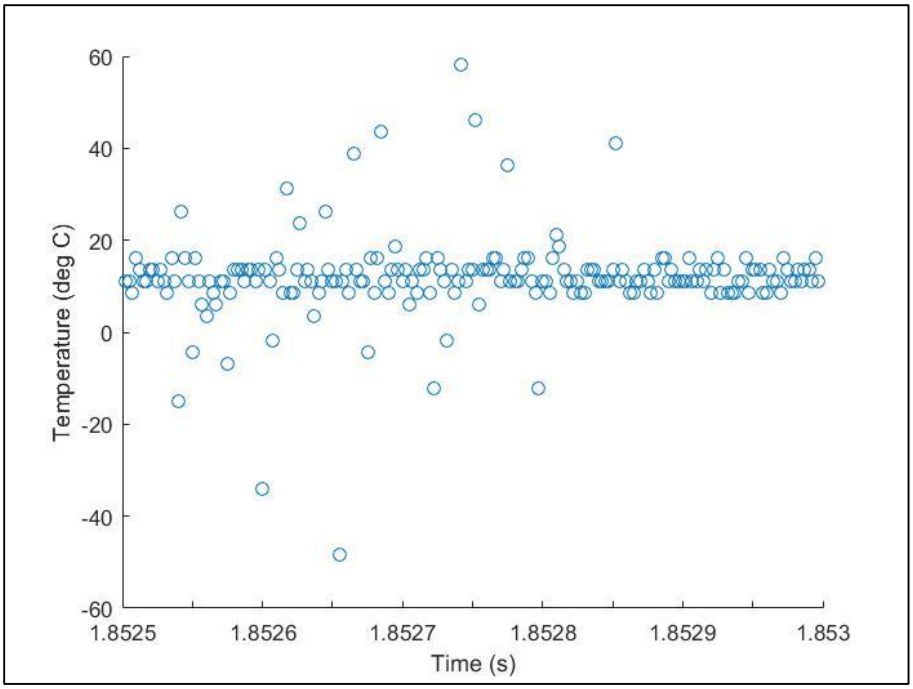

Figure 4.31: Scatter diagram of exhaust temperature at 0.5 in. from detonation tube end measured by AWG 20 thermocouple

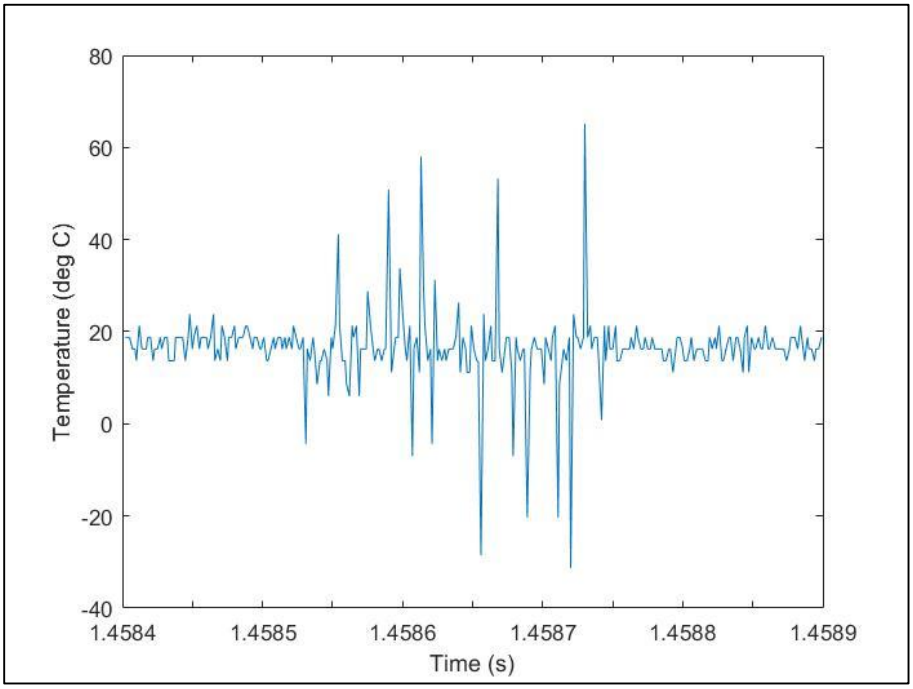

Figure 4.32: Exhaust temperature at 0 in. from detonation tube end measured by AWG 20 thermocouple

The initial experiment started off by keeping the probe at 6.25 in. from the detonation tube open end. The temperature recorded was very low than the stipulated temperature. Hence, the probe was kept at different distances from detonation tube exhaust from just outside the tube to 2 in. from the exhaust. The temperature increased only marginally when the probe was taken closer to the detonation tube. Figure 4.32 depicts the temperature profile from another dataset. The thermocouple used was again AWG 20. The probe was kept just outside the detonation tube. But, still the maximum temperature recorded was 64 ^{0}C.

AWG 24 thermocouple is another thermocouple which was calibrated. The time constant of the step temperature response of AWG 24 was found to be better than AWG 20 thermocouple. Hence, the AWG 20 thermocouple was replaced by AWG 24 thermocouple. The thermocouple probe was kept at 0.25 in. from the detonation tube exhaust. As shown in Figure 4.33, the maximum temperature recorded was 80 ^{0}C. The temperature registered by the thermocouple followed the same trend and the temperature did not improve considerably.

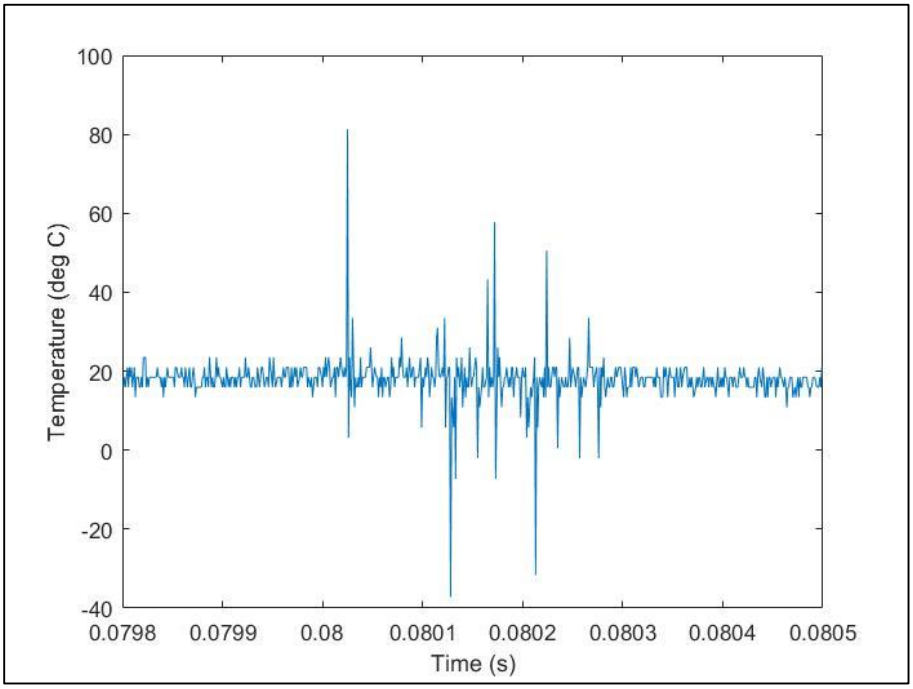

Figure 4.33: Exhaust temperature at 0 in. from detonation tube end measured by AWG 24 thermocouple

AWG 50 thermocouple was found to be the most sensitive thermocouple amongst the calibrated thermocouples. The probe making process for AWG 50 thermocouple has been explained in Chapter 1. Due to the delicate nature of thermocouple, the stagnation tube, which houses the thermocouple probe was kept at 0.75 in. from the detonation tube. The tip of the thermocouple was 1 inch away from the stagnation tube entrance. The pulse detonation engine was run with the help of modified LabVIEW program. This program allowed the number of pulses the engine can run for. Hence, the program was altered to make sure that PDE runs only for a single pulse. This was done because of the delicate nature of the thermocouple.

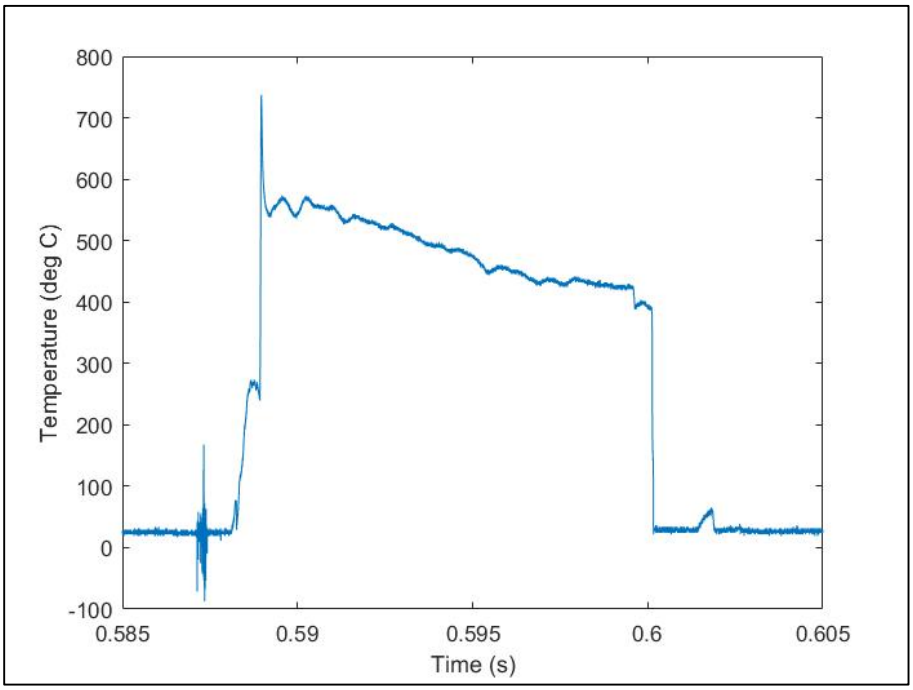

Figure 4.34: Exhaust temperature at 0.5 in. from detonation tube end measured by AWG 50 thermocouple

Figure 4.34 depicts the temperature response of the AWG 50 thermocouple. The stagnation tube was 0.5 in. from the detonation tube. The tip of the thermocouple was 1.5 in. away from the detonation tube open end. Maximum temperature recorded was 732 ^{0}C. This temperature was an improvement over the temperatures previously recorded by AWG 20 and AWG 24 thermocouples. The scatter diagram of the same is given in Figure 4.35.

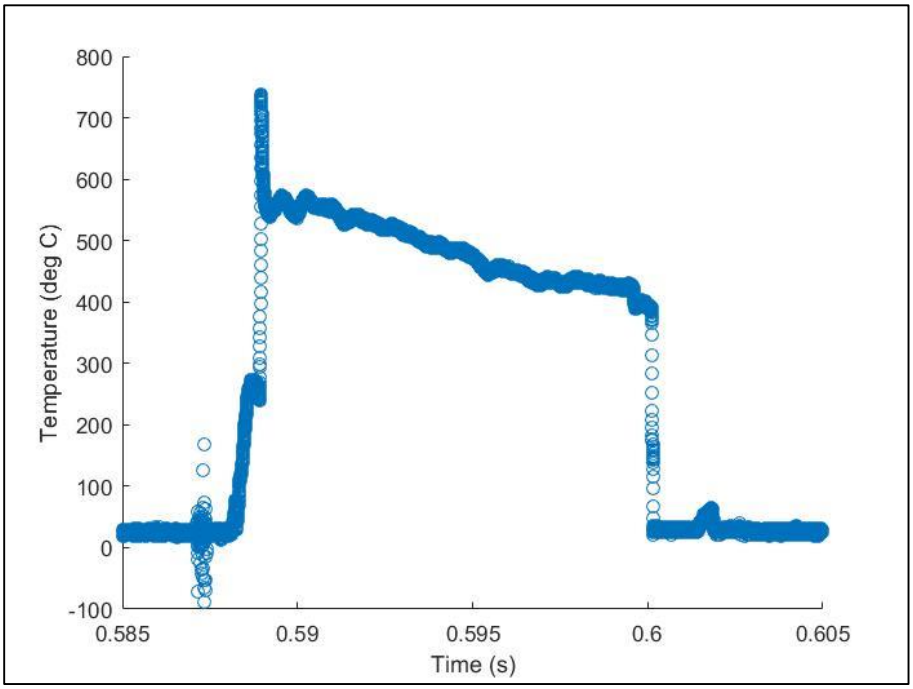

Figure 4.35: Scatter plot of exhaust temperature at 0 in. from detonation tube end measured by AWG 50 thermocouple

The sampling rate for this particular dataset was 880,000 samples per second. The high sampling rate enabled me in capturing the thermocouple response. The temperature spike around 0.587 s in Figure 4.35 is because of stress waves that propagate before the actual shock wave. The same phenomenon has been seen in few other datasets as well. Figure 4.36 and 4.37 illustrates the response of AWG 50 thermocouple from another dataset. The maximum temperature recorded in this case is 737 ^{0}C. This dataset was also recorded at the sampling rate of 880,000 samples per second.

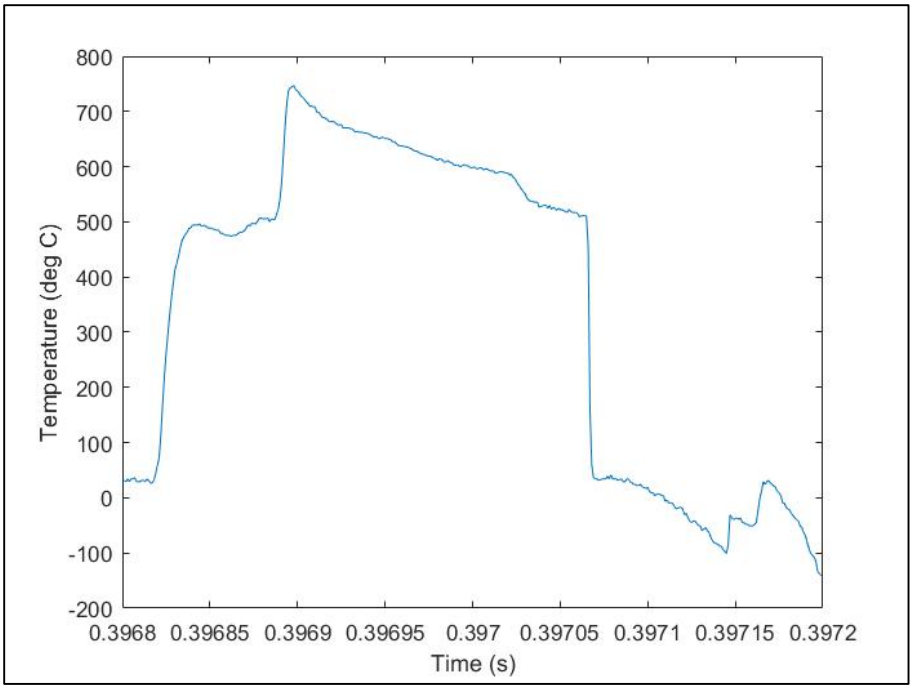

Figure 4.36: Exhaust temperature at 0.5 in. from detonation tube end measured by AWG 50 thermocouple

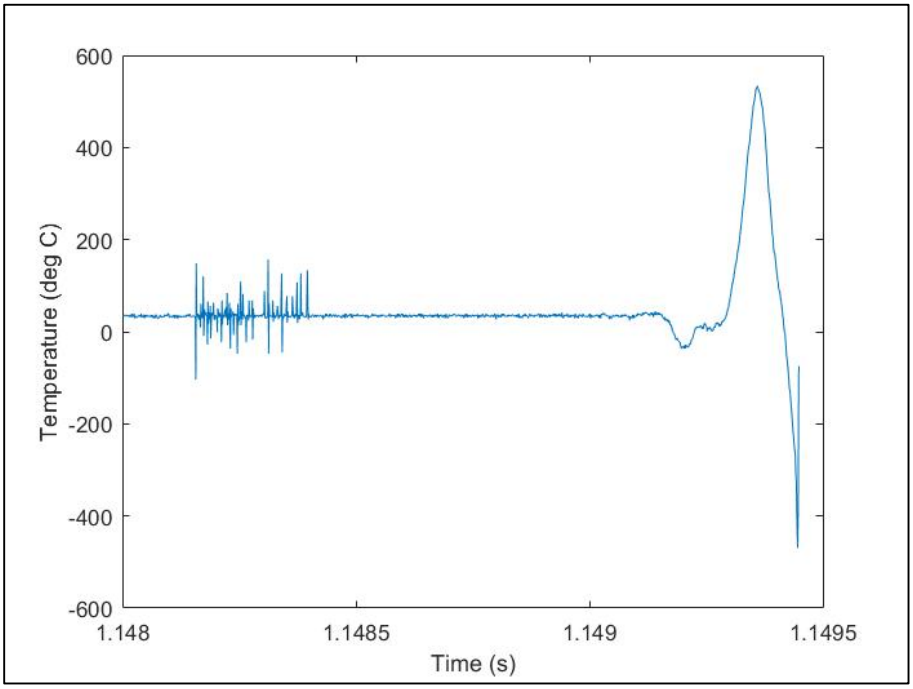

Figure 4.37: Exhaust temperature at 0.5 in. from detonation tube end measured by AWG 50 thermocouple

It was feared that due to the delicate nature of the thermocouple, it will not be able to survive multiple impacts of detonation wave. But, the thermocouple was still intact after 15 runs at 0.75 in. away from the detonation tube and 14 runs at 0.5 in. away from the detonation tube exhaust. Hence, the thermocouple was moved closer towards the detonation tube. Figure 4.38 shows the temperature rise recorded by the thermocouple at 0.25 in. away from the detonation tube open end. The maximum temperature recorded was 530 ^{0}C. The stress wave phenomenon can be seen between 1.1482 and 1.1484 s. The sampling rate for all the datasets, which were recorded for the thermocouple position at 0.25 in., were at 880000 samples per second.

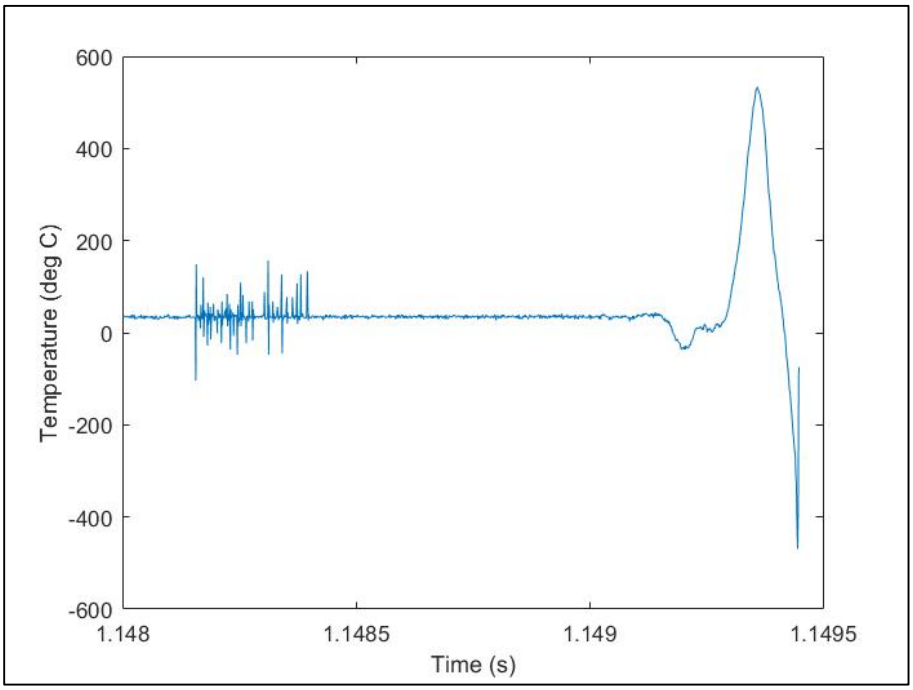

Figure 4.38: Exhaust temperature at 0.25 in. from detonation tube end measured by AWG 50 thermocouple

Figure 4.38 shows the temperature rise recorded by the thermocouple at 0.25 in. away from the detonation tube open end. The Figure belongs to dataset 2. The maximum temperature recorded was 846 ^{0}C. The stress wave phenomenon (not shown in Figure 4.39) was observed between 0.9219 and 0.9222 s.

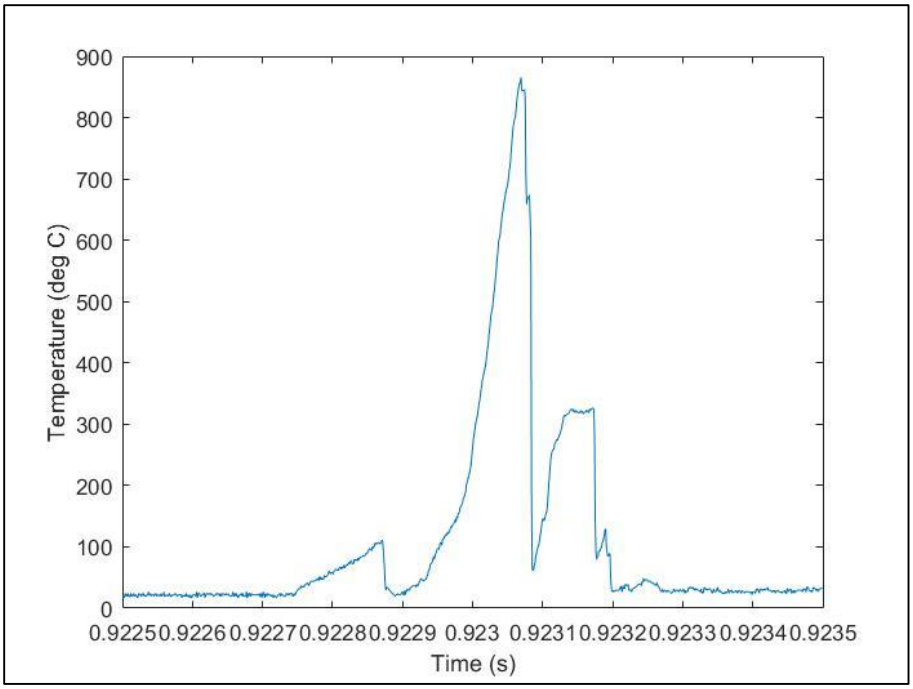

Figure 4.39: Exhaust temperature at 0.25 in. from detonation tube end measured by AWG 50 thermocouple

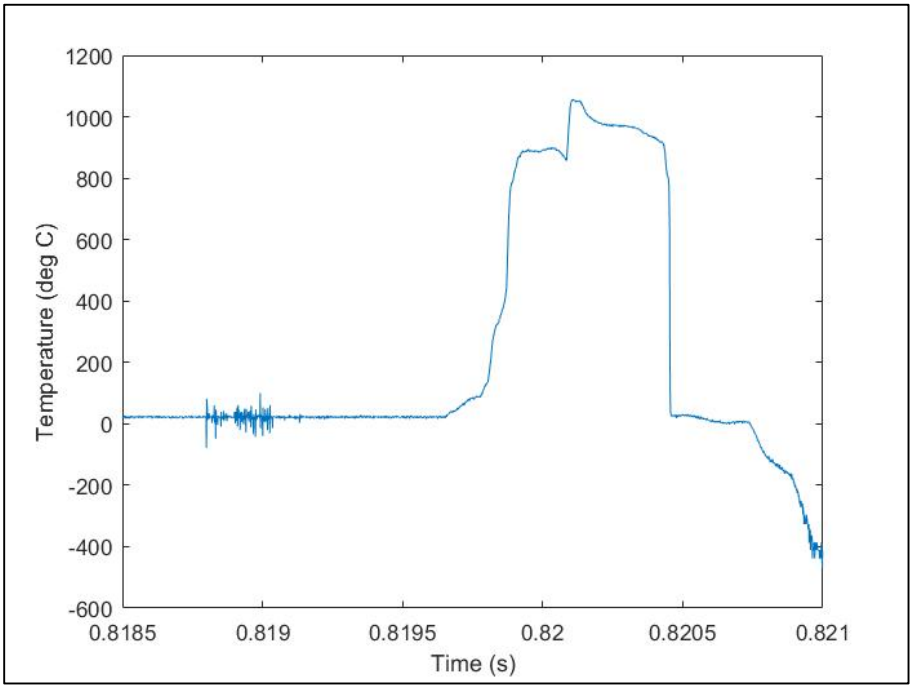

Figure 4.40: Exhaust temperature at 0.25 in. from detonation tube end measured by AWG 50 thermocouple

Figure 4.40 shows the maximum temperature rise recorded by AWG 50 thermocouple amongst all the datasets. The thermocouple was at 0.25 in. away from the detonation tube exhaust end. The maximum temperature recorded was 1049 ^{0}C. The stress wave phenomenon was observed between 0.8188 and 0.819 s.

4.4– Total Temperature Measurement [10]

The temperature measured at the exhaust of the PDE cannot be directly used for further calculations and different corrections need to be applied to it.

4.4.1 Recovery Factor

The overall recovery factor can be defined as the difference between measured temperature and total temperature of the gas. The recovery factor is an amalgamation of the velocity error which is related to the adiabatic temperature recovery along with the conduction and convection losses of the temperature from the probe.

4.4.2 Velocity Error

The temperature that should be measured by the thermocouple when it is placed inside a stagnation tube, is total temperature. As the process of stagnating the gas is not isentropic, there is always the heat dissipation through the frictional means when the gas comes in contact with the thermocouple probe.

4.4.3 Radiation Error

The radiative heat transfer occurring between the hot jet which is coming from the detonation tube and the surrounding can be a major reason for difference between the actual temperature and the measured one.

To compute the total temperature the corrected temperature is then substituted in equation (1.7), which can be given as,

$$\frac{T_0}{T} = 1 + \frac{\gamma - 1}{2} M^2$$

As the measured temperature and the computed exhaust temperature vary by great margin, further calculation for total temperature determination were not performed.

4.5– Conclusions and Future Work

- The calibration technique was devised for the thermocouples which were used for temperature measurement.
- It was observed that the time constant for thermocouples AWG 20 and AWG 24 lies between 0.05 to 0.1 s although AWG 24 thermocouples are quicker than AWG 20 thermocouples.
- AWG 50 thermocouples were quickest of the lot with the time constant between 0.001 and 0.003 s.
- It can be concluded that the exhaust pressure reduces nonlinearly as the detonation wave travels away from the detonation tube.
- AWG 20 and AWG 24 thermocouples were not able to capture temperature rise occurring due to shock wave propagation.
- Only stress wave phenomenon was captured by AWG 20 and AWG 24 thermocouples.
- AWG 50 thermocouples successfully captured temperature rise occurring due to stress waves as well as due to shock waves.
- Maximum temperature recorded was 1049 ^{0}C at 0.25 in. away from the detonation tube exhaust although the measured temperature and the calculated temperature vary by more than 2000 ^{0}C.
- It has been speculated that the difference between the temperatures is because of isentropic cooling of the jet fume.
- It is being hypothesized that the radiation losses are major reason for the loss of heat.
- A shield over the detonation tube exhaust is being proposed to mitigate the temperature loss due to radiation.

References

[1] Kailasanath, K., “Recent Developments in the Research on Pulse Detonation Engines," AIAA Journal, Vol. 41, No. 2, 2003, pp. 145-159.

[2] Roy, G.D., Frolov, S.M., Borisov, A.A., and Netzer, D.W, “Pulse Detonation Propulsion: Challenges, Current Status, and Future Perspective," Progress in Energy and Combustion Science, Vol. 30, No. 6, 2004, pp. 545-672.

[3] Lu, F.K, “Prospects for Detonation Propulsion," invited lecture, 9th International Symposium on Experimental and Computational Aerothermodynamics of Internal Flows, September 811, 2009, GyeongJu, Korea, 2010.

[4] Glassman Irvine, Yetter Richard, Combustion, 3rd Edition, Elsevier, Massachusetts, 2008.

[5] Anderson John, Modern Compressible Flow: With Historical Perspective, 2nd Edition, McGraw-Hill, 2009.

[6] Bontragger P J, “Development of Thermocouple -Type Total Temperature Probes in The Hypersonic Flow Regime," AEDC-TR-69-25, 1969.

[7] “Type E thermocouple response time and temperature coefficients”, http://srdata.nist.gov/its90/type_e/0to300.html , accessed April 11, 2015.

[8] Joshi Dibesh, “The Unsteady Thrust Measurement Techniques for Pulsed Detonation Engines,” Ph.D. Dissertation, University of Texas at Arlington, 2014.

[9] Pointwise™ Tutorial Workbook, Pointwise Inc., 2015.

[10] Villafañe Laura, Paniagua Guillermo, “Aero-thermal analysis of shielded fine wire thermocouple probes”, International Journal of Thermal Sciences, 2012.

[11] NASA CEA applet for normal shock relations, https://cearun.grc.nasa.gov

[12] Virginia Tech ‘Compressible Aerodynamics Calculator’ for normal shock relations,

http://www.dept.aoe.vt.edu/~devenpor/aoe3114/calc.html

Biographical Information

Ninad Kawle was born and raised in Mumbai, India. He received his Bachelors' of Engineering in Mechanical Engineering from University of Mumbai, India in 2012. He worked at Mahindra and Mahindra, an India based MNC, from 2012 to 2014. He began work on his Masters' of Science in Mechanical Engineering in Fall 2014 at the University of Texas at Arlington, Arlington, Texas.